

Cost Effective Emissions and Minor Species Predictions via Coupling of Computational  
Fluid Dynamics and Chemical Reactor Network Analysis

Sam Ghazi-Hesami

A Thesis

In

The Department

Of

Mechanical and Industrial Engineering

Presented in Partial Fulfillment of the Requirements

for the Degree of Master of Applied Science (Mechanical Engineering) at

Concordia University

Montréal, Québec, Canada

March 2009

© Sam Ghazi-Hesami, 2009



Library and Archives  
Canada

Published Heritage  
Branch

395 Wellington Street  
Ottawa ON K1A 0N4  
Canada

Bibliothèque et  
Archives Canada

Direction du  
Patrimoine de l'édition

395, rue Wellington  
Ottawa ON K1A 0N4  
Canada

*Your file* *Votre référence*  
ISBN: 978-0-494-63251-2  
*Our file* *Notre référence*  
ISBN: 978-0-494-63251-2

**NOTICE:**

The author has granted a non-exclusive license allowing Library and Archives Canada to reproduce, publish, archive, preserve, conserve, communicate to the public by telecommunication or on the Internet, loan, distribute and sell theses worldwide, for commercial or non-commercial purposes, in microform, paper, electronic and/or any other formats.

The author retains copyright ownership and moral rights in this thesis. Neither the thesis nor substantial extracts from it may be printed or otherwise reproduced without the author's permission.

**AVIS:**

L'auteur a accordé une licence non exclusive permettant à la Bibliothèque et Archives Canada de reproduire, publier, archiver, sauvegarder, conserver, transmettre au public par télécommunication ou par l'Internet, prêter, distribuer et vendre des thèses partout dans le monde, à des fins commerciales ou autres, sur support microforme, papier, électronique et/ou autres formats.

L'auteur conserve la propriété du droit d'auteur et des droits moraux qui protègent cette thèse. Ni la thèse ni des extraits substantiels de celle-ci ne doivent être imprimés ou autrement reproduits sans son autorisation.

---

In compliance with the Canadian Privacy Act some supporting forms may have been removed from this thesis.

While these forms may be included in the document page count, their removal does not represent any loss of content from the thesis.

Conformément à la loi canadienne sur la protection de la vie privée, quelques formulaires secondaires ont été enlevés de cette thèse.

Bien que ces formulaires aient inclus dans la pagination, il n'y aura aucun contenu manquant.

  
**Canada**

## ABSTRACT

The progress in recent years and the advent of new powerful computers have allowed experts to simulate combustion-turbulence interaction reasonably well and predict temperature and velocity fields with acceptable accuracy. However, the current technology and available computer power do not suffice in predicting the concentration of minor species such as  $\text{NO}_x$  and CO. As the reduction of these pollutants requires expensive experimentation, much attention has been directed towards more cost effective ways of simulating pollution emission via numerical methods. This research project has been conducted in order to obtain a universal cost effective method for predicting emissions via a system of Chemical Reactor Networks (CRN). This was achieved via coupling of CFD-CRN. While CFD provided temperatures, residence time and major species' concentrations, CRN was able to accurately tackle the complex chemical kinetics for prediction of minor species on a personal computer; A task which would have taken months via CFD on a computer cluster. RANS and LES simulations of an industrial Rolls Royce RB211 combustor were performed with and without Discrete Phase Modeling. CRNs were then extracted from the CFD field based on temperature, composition and geographical location via an efficient coded algorithm. It is demonstrated that the chemical kinetic computation based on the extracted CRNs from CFD provides reasonable results compared with experimental data on some of the CO predictions. It is strongly believed that higher resolutions of reactors will at least provide reasonable trends upon boundary condition variations. The algorithm developed in this study leads to a more universal approach for cost effective prediction (quantitatively or qualitatively) of combustion emissions, which contribute to cardiovascular and respiratory ailments.

## ACKNOWLEDGMENTS

I am grateful to Dr Pierre Gauthier and Dr Marius Paraschivoiu who have kindly and patiently supervised and supported me throughout the course of my research. I also thank Dr Hoi Dick Ng for joining my panel of supervisors towards the end of my thesis and giving me invaluable help and advice. I thank Rolls Royce Canada and Dr Bourque from Rolls Royce Canada for giving me the opportunity to conduct this research.

I am most grateful to God and my parents (Fariba and M.Reza) for giving me life and constantly reminding me that with enough commitment, things can always be turned around for the best. I extend my appreciation to my brother, Surena, who has always been there for me. I dedicate this thesis to the memory of my grandparents who do not live among us anymore. I am also most grateful to my aunts and uncles (Afsaneh, Hengameh , Hydeh, Ali Hesami, Amir Hesami, Reza Hesami,) and the rest of my family for their constant support.

The content of this thesis have been removed where advised by Rolls Royce Canada to avoid publication of copy righted material.

I am also grateful for all my friends who have supported me until here and my friend and colleague Sandeep Jella who has helped me throughout this thesis. I would like to extend my thanks to Dr Kadem, Dr Vatistas, Dr Ghaly and Dr Grogono for teaching me and the technical staff at Concordia University who have maintained the computing resources required for this research.

Finally, I would like to thank Van Houtte for providing me with cheap coffee to work and Reggie's for providing me cheap drinks to celebrate my time at Concordia University!!!

*To the memory of my grand mothers;*

# CONTENTS

1	INTRODUCTION .....	1
1.1	Summary .....	5
2	FUNAMENTALS OF CHEMICAL REACTOR NETWORK MODELING .....	6
2.1	Types of Chemical Reactors .....	6
2.1.1	PSR (Perfectly Stirred Reactor) .....	7
2.1.2	PFR (Plug Flow Reactor) .....	7
2.1.3	PaSR (Partially Stirred Reactor) .....	8
2.2	Conservation Laws and CRN Theory .....	8
2.2.1	Conservation Laws for a Perfectly Stirred Reactor .....	9
2.2.2	Conservation Laws for a Plug Flow Reactor .....	11
2.3	Description of Chemkin .....	12
2.3.1	CRN Validation using Chemkin .....	13
2.3.2	Chemical Reaction Mechanism (GRI 1.2 vs GRI 3.0) .....	14
2.3.3	Mechanism Interaction .....	15
2.4	Summary .....	17
3	FLOW FIELD DISCRETIZATION METHODOLOGY .....	18
3.1	From CFD to CRN: Traditional Approaches .....	18
3.1.1	Method I .....	21
3.1.2	Method II .....	23
3.1.3	Method III .....	24
3.2	From CFD to CRN: Current Approach .....	25
3.3	Mixture Fraction and Temperature .....	28
3.4	Zone of Influence .....	32
3.5	Volume and Residence Time .....	34
3.6	Flow Mass Split .....	36
3.7	Removal of Small Reactor .....	38
3.8	Addition of Cooling Air via Source Terms .....	39
3.9	CFD-CRN Generation Algorithm Flow Chart .....	40
4	ALGORITHM APPLICATIONS .....	44
4.1	CFD Simulation of an RB211 Combustor .....	46
4.2	CFD Simulation of Simpler Models .....	52
4.3	Reactor Generation .....	54
4.3.1	Description of Input File .....	54
4.3.2	Graphical Display .....	58
4.4	Reactor Networks in Chemkin .....	60
4.5	Summary .....	65
5	RESULTS .....	66

5.1	CRN Simulation of the Lockwood Combustor.....	66
5.2	CRN Simulation of the RB211 Combustor's 45 Degree Slice.....	68
5.3	CRN Simulation of the Full RB211 Combustor.....	72
5.4	NO <sub>x</sub> Emission .....	78
5.5	CO Emission.....	81
5.6	Summary.....	83
6	CONCLUSION.....	84
6.1	Future Work.....	88
6.2	Contribution to Knowledge.....	90
	REFERENCE.....	91
	APPENDIX A-FLUX CALCULATIONS .....	97
	APPENDIX B-TRIMMING OF REACTORS .....	98
	APPENDIX C-CRN SIMPLIFIED.....	100

## FIGURES

Figure 3-1: Image of the primary zone of the combustor with virtual PSRs.....	20
Figure 3-2: Based on the streamlines, cells are grouped to represent PFRs in series and parallel <sup>(23)</sup> .....	21
Figure 3-3: Representation of a reactor network for a LP combustor (Andreini et al <sup>(25)</sup> )	24
Figure 3-4: Depiction of refined reactor resolution (left) and original resolution of reactors around the flame (right).....	31
Figure 3-5: A sample of the flow field discretization within each ZoI on a RB211 RANS model.....	33
Figure 4-1 A representation of the programming phases of the developed algorithm for RB211 analysis .....	45
Figure 4-2: 2D portrayal of velocity vectors and the premixer grid .....	48
Figure 4-3: Sample of the mesh used.....	49
Figure 4-4: 3D complex mesh on RB211 .....	50
Figure 4-5: Premixer and secondary windows' mesh.....	51
Figure 4-6: Lockwood geometry .....	52
Figure 4-7: RB211 combustor 45 degree slice .....	53
Figure 4-8: Input file heading .....	55
Figure 4-9: Input file part I .....	55
Figure 4-10: Input file part II.....	56
Figure 4-11: Input file part III.....	57
Figure 4-12: Input file part IV .....	58
Figure 4-13: Eleven 3D reactors displayed on Fluent GUI .....	59
Figure 4-14: Initial view of CRN in Chemkin's GUI.....	61
Figure 4-15: Expanded view of CRN on Chemkin's GUI.....	63
Figure 5-1: Lockwood CRN on Fluent .....	67
Figure 5-2: Lockwood CRN on Chemkin.....	67
Figure 5-3: Sample RB211 Pie slice CRN.....	69
Figure 5-4: Sample extended RB211 Pie slice with straightened discharge nozzle .....	70
Figure 5-5: RB211 CRN-species concentration .....	71
Figure 5-6: CRN on Fluent GUI and Chemkin.....	75
Figure 5-7: Sample of 3D complex full RB211 combustor's CRN.....	76
Figure 5-8: RB211 Combustor schematic (Ref 39).....	77
Figure 5-9: CRN and experimental NO <sub>x</sub> values .....	80
Figure 5-10: CRN and experimental CO values .....	82
Figure C-1: Depiction of reactors extracted from the CFD field.....	100



## NOMENCLATURE

VARIABLE	DESCRIPTION
$\rho$	Density $\left(\frac{kg}{m^3}\right)$
A	Area ( $m^2$ )
v and u	Velocity $\left(\frac{m}{s}\right)$
m	Mass (kg)
$\dot{m}$	Mass flow rate $\left(\frac{kg}{s}\right)$
$C_p$	Specific heat $\left(\frac{joules}{g.K}\right)$
T	Temperature (K)
$K_{EC}$	Equilibrium constant
$S^0$	Entropy $\left(\frac{joules}{K}\right)$
H	Enthalpy ( <i>joules</i> )
p	Pressure (Pascals)
$k_i$	Forward rate of reaction constant
$R_u$	Universal gas constant

Y	Mass fraction
V	Volume ( $m^3$ )
W	Molecular weight
C	Molar concentration ( $\frac{moles}{m^3}$ )
A	Area ( $m^2$ )
T	Temperature (K)
$T_w$	Wall Temperature (K)
$T_{ref}$	Reference Temperature (K)
$T_{ex}$	Exit Temperature (K)
$h_k$	Specific enthalpy of the $k^{th}$ species ( $\frac{J}{kg}$ )
h	Heat transfer coefficient ( $\frac{W}{m^2.K}$ )
P	Momentum vector ( $\frac{kg.m}{s}$ )
t	Time (s)
E	Energy (joule)
$Y_k^*$	Mass fraction of species k at the inlet
f	Mixture fraction

$f'$	Mixture fraction variance
$\omega$	Production/Destruction rate of species $\left( \frac{\text{moles}}{m^3 \cdot s} \right)$
CRN Generator	Refers to the name of the C program developed for the creation of chemical reactor networks
UDF	User Defined Function
UDM	User Defined Memory
CRN	Chemical Reactor Network
CFD	Computational Fluid Dynamics
Zoi	Zone of Influence
GUI	Graphical User Interface



# 1 INTRODUCTION

In recent years special attention has been directed towards modern technologies' impact on the environment and consequently human health. Health Canada summarizes the effects of air pollution to be principally on respiratory and cardiovascular systems <sup>(1)</sup>. Some of the recent initiatives such as the NO<sub>x</sub> Budget Trading Program <sup>(2)</sup> under the NO<sub>x</sub> SIP call and Ozone Transport Commission NO<sub>x</sub> Budget Program in the United States and the Kyoto Protocol <sup>(3)</sup> ratified by 180 nations show the global determination in battling the air pollution issues around the world. According to the World Health Organization, 2.4 million people die each year as a direct result of air pollution <sup>(4)</sup>.

Therefore, various initiatives have been taken to introduce more environmentally friendly sources of energy such as solar energy, wind energy, the oceans' energy and even nuclear energy. These resources suffer from their unique set backs and have been slow in replacing fossil fuel as the main source of energy. It is apparent that fossil fuels will not leave our daily lives any time soon; therefore alternative means of utilizing fossil fuel energy with minimized impact on the well being of the global village is required.

Industrial combustion contributes to roughly 18% of NO<sub>x</sub> emission in the United States based on a study in 2000 which ranks it as the second highest pollution source in the category of stationary sources. Pollution production can be altered via the choice of fuel and the method of combustion. The use of natural gas in stationary gas turbine makes

them a relatively clean source of energy. Natural gas, which is mainly composed of methane, has a high hydrogen to carbon ratio of 4 to 1 which results in its low emissions of CO. Also a lack of sulphur in natural gas eliminates the possibility of sulphur dioxide emission which is considered hazardous.

Although natural gas is a relatively clean fuel, it is still capable of producing unacceptable levels of  $\text{NO}_x$  and CO which has led the industry to seek new ways of controlling the emissions in natural gas. New combustion methods can be categorized into pre-treatment, modern combustion mechanisms and post-treatment. Catalytic treatment and fuel switching are some of the pre- and post-treatment methods currently in place. The complexity of design and manufacturing of combustion chambers requires a thorough computational analysis of the flow before producing the combustor for further experiments. Gas turbine companies have been facing new stringent emission and efficiency demands from their governments and clients. In order to meet the demand at reasonable costs, they are obliged to take advantage of modern fluid dynamic simulations to reduce the number of rig tests required. Computational Fluid Dynamics (CFD) has been used extensively for the reasons mentioned above, however, the complexity of long reaction mechanisms pose severe time penalties for detail combustion simulations<sup>(5)</sup>. The coupling of CFD-combustion interaction often takes advantage of simplified models which can predict temperature, velocity and fast species' (such as  $\text{CH}_4$ ,  $\text{O}_2$ ) concentration with reasonable accuracy while failing to predict the production of slower species such as CO and  $\text{NO}_x$ . Some attempts have been made at reducing and customizing the complex mechanisms for specific conditions in order to achieve

reasonable computational time. For example, Novoselov et al have proposed an eight step global mechanism for methane at certain conditions <sup>(6, 7)</sup>. However, effective CFD simulations still require expansive computational capacity. The complex nature of combustion processes and their comprising intermediate reactions render detail CFD turbulent combustion simulations impractical. In order to control emissions, a great deal of computational/theoretical research is being conducted to potentially predict the output emissions. The alternative in combustion simulation is believed to lie in decoupling of combustion from the CFD field. One of the potential methods is to simultaneously solve the combustion equations separately from the CFD.

The definition of a general method to estimate NO<sub>x</sub> and CO emissions in large industrial combustion systems is the principal goal of this research. The current project aims at decoupling the CFD simulation from detail chemical kinetics. The flow field information (such as temperature, composition and residence time) is transferred into a purely chemical kinetics solver which simultaneously solves the underlying governing equations. With this simplification, the simultaneous solution of the equations in a purely chemical kinetics solver with no turbulent and flow effects shall enhance the solution time by several orders of magnitude.

One method to compute the chemical kinetics is via a simplified Chemical Reactor Network (CRN). CRNs allow the user to investigate the concentration of slower species such as NO<sub>x</sub> and CO. A typical CRN comprises of a series of theoretical reactors (e.g. perfectly stirred reactor PSR, plug flow reactor PFR and partially stirred reactor PaSR)

which resemble unique parts of the CFD flow field. The simple reactors are modeled only by energy and species transport equations. Although seemingly simple, many attempts have so far failed to devise a universal method which would systematically generate a chemical reactor network representative of the CFD flow field. This thesis aims to offer a universal method of creating CFD dependent chemical reactor networks which is easy and robust to implement using the conventional CFD softwares and reasonable computing power. It also takes into account the limitations and shortcomings of the available algorithms and offers ways around them. The chemical reactor network is created based on CFD predictions of an industrial RB211 combustor. A systematic approach (that accounts for mass flow splits and residence time without the need for user adjustment) is devised to produce the desired reactor network. The reactor network generated would be of reasonable complexity considering the available computing power.

Although large reactor networks could not be used (as done by Falcitelli et al <sup>(8)</sup>) due to numerical and software limitations, Falcitelli et al's <sup>(8)</sup> systematic approach in reactor network generation has been used in the current project. Falcitelli et al generate a reactor network based on the flow field's composition and thermal characteristics as implemented in this thesis. Once the geometry is discretized according to its temperature and composition field, a representative reactor network is solved using the commercially available software "Chemkin". Due to the stiff nature of the equations and the complexity of the flow field, it is highly challenging to obtain convergence with reasonable accuracy. This requires several iterations in producing a reactor network and numerical adjustments in the solver's settings. Care must be taken to avoid averaging over large thermal and



compositions gradients and to avoid generating small reactors which would only pose further convergence difficulties without playing a major role in the solution of the flow field. Averaging over large gradients can also result in unreasonable predictions of species' concentration.

## **1.1 Summary**

The negative effects of pollutants caused by combustion have been recognized. There has been a tendency towards using cleaner sources of energy such as the natural gas.

However, new methods of emissions prediction are vital to design environmentally friendly combustion chambers. Currently, CFD simulations require unfeasible amount of computing power to predict minor species' concentrations. Since CFD simulations are capable of predicting temperature and flow field properties with reasonable accuracy, a novel method is proposed and implemented by decoupling the chemical kinetics involved from the CFD flow field. Decoupling of chemical kinetics from CFD allows tackling of large combustion mechanisms and calculation of minor species within a short period of time with limited computing power. The goal is to devise a method that allows quantitative or at least qualitative prediction of emissions with reasonable accuracy within a reasonable time frame and using the available computing power.

## **2 FUNAMENTALS OF CHEMICAL REACTOR**

### **NETWORK MODELING**

The current study is to model the CFD flow field solution by a chemical reactor network which can predict emissions with reasonable accuracy or can at least predict the trend in emissions production with changes in the flow field. A chemical reactor network is comprised of a series of theoretical reactors. In this Chapter, the basic CRN theory including different types of reactors and their mathematical models are reviewed and discussed. The commercial software Chemkin, which is capable of carrying out CRN computations, is introduced.

#### **2.1 Types of Chemical Reactors**

Traditionally, chemical reactor network typically consists of the following types of reactor element combinations.

### **2.1.1 PSR (Perfectly Stirred Reactor)**

The PSR can be defined in terms of a PFR cut into a number of small sections where each section has an almost uniform temperature and composition. The Perfectly Stirred Reactor (PSR) or the Continuously Stirred Tank Reactor (CSTR) which has been utilized extensively for academic and industrial purposes is an ideal reactor within which the temperature and composition are uniform throughout due to the instant mixing of the incoming flow. The reactor composition can change over time but not over space. Kee et al <sup>(9)</sup> describe the instantaneous perfect mixing to be due to high molecular diffusion (for example at low pressures) or high turbulence intensity. The state of the mixture is determined based on the temperature, composition and residence time of the flow. In theoretical models, one could fix the temperature in the reactor if the main concern is to study reaction chemistry while neglecting the energy balance. The temperatures are usually extracted from a CFD analysis or experimental data.

### **2.1.2 PFR (Plug Flow Reactor)**

Annamalai et al <sup>(10)</sup> define the PFR to be “a reactor in which there is no radial variation of the system properties”. Plug flow reactors are one-dimensional reactors where the flow composition and thermodynamic state can vary along the flow path but not radially. It must be noticed that also the diffusive transport is neglected along the flow direction.

### **2.1.3 PaSR (Partially Stirred Reactor)**

One of the other elements which may be considered for use in the future is the partially stirred reactor. As the name indicates, this reactor differs from the PSR due to its mixing. In many industrial applications such as gas turbines and internal combustion engines, the mixing is not always fast enough for the flow to represent a PSR. Therefore, the partially stirred reactor could offer a more realistic approach by taking unmixedness into account<sup>(11, 12)</sup>. The thermo chemical properties of a PaSR are homogeneous spatially while maintaining some unmixedness on the molecular level. This unmixedness is usually fed into the reactor in terms of mixing frequency or eddy turn over time. A choice of mixing models is also available<sup>(12)</sup>. While PSRs and PFRs can take the fluid flow field information via the residence time only, partially stirred reactors can take more of the flow field information via the residence time and unmixedness.

## **2.2 Conservation Laws and CRN Theory**

The mathematical formulation in CRN modeling turns the complex CFD problem into a purely kinetics problem and allows the user to solely focus on the reactions involved in the combustion field. In this section a summary of the main equations involved in solving of a reactor network are described.

## 2.2.1 Conservation Laws for a Perfectly Stirred Reactor

The species conservation equation for the  $k^{\text{th}}$  species can be written as;

$$\left(\frac{dm_k}{dt}\right)_{\text{system}} = \int_{CV} \dot{\omega} W_k dV \quad \text{Equation 2.1}$$

The right hand side would indicate the production or the consumption of the species.

Therefore, the integration over the control volume would expand the equation to;

$$\int_{CV} \frac{\partial}{\partial t} (\rho Y_k) dV + \int_{CS} \rho Y_k V \cdot n dA = \int_{CV} \dot{\omega}_k W_k dV \quad \text{Equation 2.2}$$

It may be worthwhile to point out that the species equation (Equation 2.2), when applied to large chemical mechanisms for complex mass flow splitting, generates very stiff matrices. In simple words, stiff equations require a much smaller time step to remain stable compared with the time step they require to maintain accuracy. Special numerical treatment, smaller time steps, and frequent updating of the Jacobian are used to achieve convergence. Kee et al <sup>(9)</sup> address the treatment of stiff equations in full detail.

For a fixed volume of uniform properties the integration over the volume would simplify

the equation further to;

$$\frac{\partial(\rho Y_k)}{\partial t} V + \int_{CS} \rho Y_k V \cdot n dA = \dot{\omega}_k W_k V \quad \text{Equation 2.3}$$

The details of the mathematical derivation could be found in Ref 9. The final derivation of the species conservation equation for the perfectly stirred reactor is;

$$\frac{dY_k}{dt} = \frac{\dot{m}}{\rho V} (Y_k^* - Y_k) + \frac{\dot{\omega}_k W_k}{\rho} \quad \text{Equation 2.4}$$

The energy equation can be simplified by neglecting the kinetic and potential energy due to gravity. The energy equation in its general form can then be written as follows;

$$\left( \frac{dE}{dt} \right)_{system} = \frac{dQ}{dt} + \frac{dW}{dt} \quad \text{Equation 2.5}$$

The Reynold's transport theorem could be used to transform the equation in its general form into;

$$\int_{CV} \frac{\partial}{\partial t} (\rho e) dV + \int_{CS} \rho e V \cdot n dA = \dot{Q} - \int_{CS} p V \cdot n dA \quad \text{Equation 2.6}$$

where  $h = e + \frac{p}{\rho}$  and  $\dot{Q}$  is the heat crossing the control surface.

The enthalpy definition could be incorporated into the above equation to derive a more comprehensive equation.

$$\int_{cv} \frac{\partial}{\partial t} (\rho e) dV + \int_{cs} h p V \cdot n dA = \dot{Q}$$

*Equation 2.7*

Notice that a positive  $\dot{Q}$  indicates heat being transferred to the reactor.

The energy equation can be finalized as follows;

$$c_p \frac{dT}{dt} = \frac{m}{\rho V} \sum_{k=1}^K Y_k^* (h_k^* - h_k) - \sum_{k=1}^K \frac{h_k \dot{W}_k}{\rho} + \frac{\dot{Q}}{\rho V}$$

*Equation 2.8*

## 2.2.2 Conservation Laws for a Plug Flow Reactor

The plug flow reactor is always used in steady state for the current project's purpose. The general conservation laws are similar to the ones already defined for the case of perfectly stirred reactors. Therefore only the equations in their final forms are written here.

The continuity equation for the perfectly stirred reactor can be finalized as;

$$\rho u \frac{dY_k}{dz} = \dot{\omega}_k W_k \quad \text{Equation 2.9}$$

The energy equation in its final format can be written as;

$$\rho u c_p \frac{dT}{dz} = \frac{\hat{h}P}{A_c} (T_w - T) - \sum_{k=1}^K h_k (\dot{\omega}_k W_k) \quad \text{Equation 2.10}$$

where;

$$h = \sum_{k=1}^K Y_k h_k \quad \text{Equation 2.11}$$

$$c_p = \sum_{k=1}^K Y_k c_{p,k} \quad \text{Equation 2.12}$$

$$\dot{m} = \rho A_c u \quad \text{Equation 2.13}$$

$$\rho = \frac{p \bar{W}}{RT} \quad \text{Equation 2.14}$$

## 2.3 Description of Chemkin

These conservation equations are the backbone of chemical kinetics solver. Temperature, species mole fraction, pressure and volume are the main variables required in solving these equations. This information is extracted from a CFD flow field and is written in a format recognizable by Chemkin to perform the subsequent kinetic analysis.



Chemkin is a software provided by Reaction Design which specializes in calculation of reactive flow systems. It was originally provided by Sandia National Laboratory as an open source software but was later purchased by Reaction Design and is currently a commercial software.

Chemkin is made up of 5 major infrastructural subroutines for: 1) gas phase chemical kinetics 2) transport properties 3) surface kinetics 4) two point boundary value solver and 5) the thermodynamic data base.

It was originally devised as a simple chemical kinetics solver and contained basic reactor models such as the perfectly stirred reactor and the plug flow reactor. Today it is a high-tech software and includes highly specialized models such as the partially stirred reactor model with PDF and mixing models.

This software was chosen due to its long history of validation, robustness and technical support.

### **2.3.1 CRN Validation using Chemkin**

Since the information available on chemical reactor networks and Chemkin is relatively scarce compared with CFD and Fluent applications, it was decided to examine Chemkin's results with an experiment. The experiment by Rutar et al<sup>(13)</sup> was therefore chosen where

they simulate a PSR behaviour using a high pressure jet stirred reactor at a very short residence time of 0.5 ms. The pressure and temperature were held at 6.5 atm and 1825 K respectively. It must be noticed that according to Rutar et al <sup>(14)</sup> the NO<sub>x</sub> reduction with pressure is *only noticeable* for pressures of up to 5 atm and almost negligible at pressures over 7 atm at a temperature of 1825 K. Therefore there is reasonable correspondence to a typical industrial combustor's operating conditions *in terms* of NO<sub>x</sub> production *sensitivity*. The mass flow rate was adjusted to simulate a residence time of 0.5 ms at a volume of 1.5 cm<sup>3</sup> corresponding to Rutar's experiment. However Keller et al <sup>(15)</sup> indicate that NO<sub>x</sub> and CO production is not a systematic function of the mass flow rate as long as the equivalence ratio is held constant for lean mixtures.

Chemkin calculations estimate the NO concentration to be at  $1.39 \times 10^{-5}$  and a water mole fraction of 0.15 which corresponds to about 16 ppm NO. NO<sub>2</sub> mole fraction is on the order of  $10^{-8}$  and is almost negligible. The NO<sub>x</sub> was then corrected to 15% oxygen <sup>(16)</sup> and the corrected NO<sub>x</sub> was calculated to be 5 ppm which closely corresponds to the measured value <sup>(13)</sup>.

### **2.3.2 Chemical Reaction Mechanism (GRI 1.2 vs GRI 3.0)**

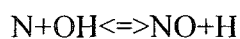
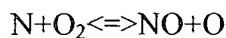
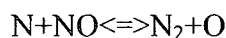
To reduce the numerical weight on Chemkin a few initial trials on the CRN were carried out with GRI 1.2 which is slightly less developed than GRI 3.0. Sensitivity analysis in an equilibrium model <sup>(12)</sup> was implemented to see the difference between the two reaction mechanisms. The GRI 1.2 showed a consistent over prediction of equilibrium

temperature by about 5 degrees over all the air fuel ranges which is not significant. This may be justified by a lack of endothermic reactions in the simpler GRI 1.2 model however the difference is not significant. The final simulations in this thesis were however implemented with the full GRI 3.0.

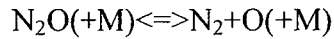
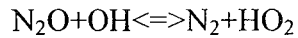
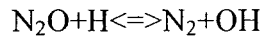
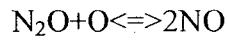
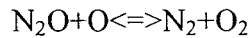
### 2.3.3 Mechanism Interaction

It was realized that for the understanding of the role of each NO<sub>x</sub> production route, a sensitivity analysis is required to determine the amount of interaction between the major NO<sub>x</sub> producing reaction paths in the GRI 3.0. The developers of the GRI mechanism recommend that the mechanism has to be used as a whole and any changes may result in inaccuracies<sup>(17)</sup>.

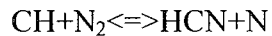
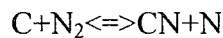
Based on the work of Guo et al<sup>(18)</sup> it was decided to modify the GRI 3.0 to account for only one of NO formation path at a time. Therefore, for the thermal Zel'dovich mechanism the following routes were disabled based on Ref 9.



The N<sub>2</sub>O path was recognized and disabled based on the work of Steele et al<sup>(19)</sup>. The following paths were singled out.



Two reactions categorized by Kee et al <sup>(9)</sup> as the most important initiating prompt reactions were disabled. These reactions are:



From the available literature, it was assumed that three main routes contribute to the  $\text{NO}_x$  formation and these are  $\text{N}_2\text{O}$  intermediate, thermal Zel'dovich and prompt mechanisms. As a sensitivity analysis each path was run individually and the  $\text{NO}$  production was later added up to see the disparity between the full GRI and the modified GRI in order to evaluate the interaction effects. The sensitivity analysis was done on an 8 reactor CRN model of a 45 degree RB211 primary zone model.

The average disparity between the  $\text{NO}_x$  produced by using the full GRI 3.0 and the  $\text{NO}_x$  calculated by the addition of each  $\text{NO}_x$  producing mechanism was calculated to be 6.72%. The average 6.72% corresponds with the work of Guo et al <sup>(18)</sup> who predicted a

4% disparity due to a lack of interaction in their laminar premixed flame models.

## **2.4 Summary**

In this chapter the concept of Chemical Reactor Networks (CRN), their composing elements and the governing equations have been introduced. It was shown that the chemical kinetics could be separated from the flow and solved more efficiently in a kinetics solver package. The current software Chemkin has been introduced due to its simplicity and available technical support. Validations on the software performance and the GRI mechanisms have been done to show the adequacy of Chemkin for the current project.

### **3 FLOW FIELD DISCRETIZATION METHODOLOGY**

Many attempts have so far failed to devise a universal method which would systematically generate an accurate chemical reactor network representative of the flow field. At present, there is no hard rule for the number of reactors needed. Reactor networks for various purposes vary in sophistication and complexity and they seem highly case dependent. This chapter first reviews different previous methods and then discusses the current systematic approach to generating CRN from CFD solutions.

#### **3.1 From CFD to CRN: Traditional Approaches**

Studies have been conducted since the 50s to simplify the flow field in order to concentrate the computer time on resolving the kinetics involved in combustion processes. In 1953, Bragg<sup>(20)</sup> proposed the idea of presenting a combustion chamber with a perfectly stirred and a plug flow reactor for the primary and secondary parts of the combustor. Flow properties (composition and temperature) are homogeneous within a perfectly stirred reactor while they can change axially only in a plug flow reactor. Zonal

combustion modeling was later proposed by Swithenbank <sup>(21)</sup> which set the path for the creation of more elaborate reactor networks. At present, there is no hard rule for the number of reactors needed. Reactor networks for various purposes vary in sophistication and complexity and they seem highly case dependent. While Schlegel et al <sup>(22)</sup> have used a simple combination of PSRs and PFRs in their model, Falcitelli et al <sup>(8)</sup> have used hundreds of PSRs to represent their network. Ehrhardt et al <sup>(23)</sup> have taken advantage of a large number of PFRs to represent their combustor's simple flow field. At a basic level, the experimental Jet Stirred Reactors (JSR) have been studied extensively by Rutar et al <sup>(14)</sup> in order to simulate one PSR or multiple PSRs and PFRs and the results have been validated against the experiments.

So far, the majority of reactor networks generated require the user to adjust very important factors like residence time and mass flow splits, to ensure compliance with experimental data. Only simple cases which are represented with hundreds of reactors require minimal adjustment from the user. Large reactor networks similar to that of Falcitelli et al's <sup>(8)</sup> are not justifiable due to numerical and time penalties involved in complex combustor geometries.

The transformation of a CFD flow field into a chemical reactor network requires the grouping of control volumes or cells with similar properties. Each group of control volumes or cells is assumed to behave as a perfectly stirred or a plug flow reactor. Fig 3-1 is a representation of an RB211 primary zone which is divided into several regions enclosed by the red rectangles. Each rectangle represents one perfectly stirred reactor

representing the corresponding part of the flow field.

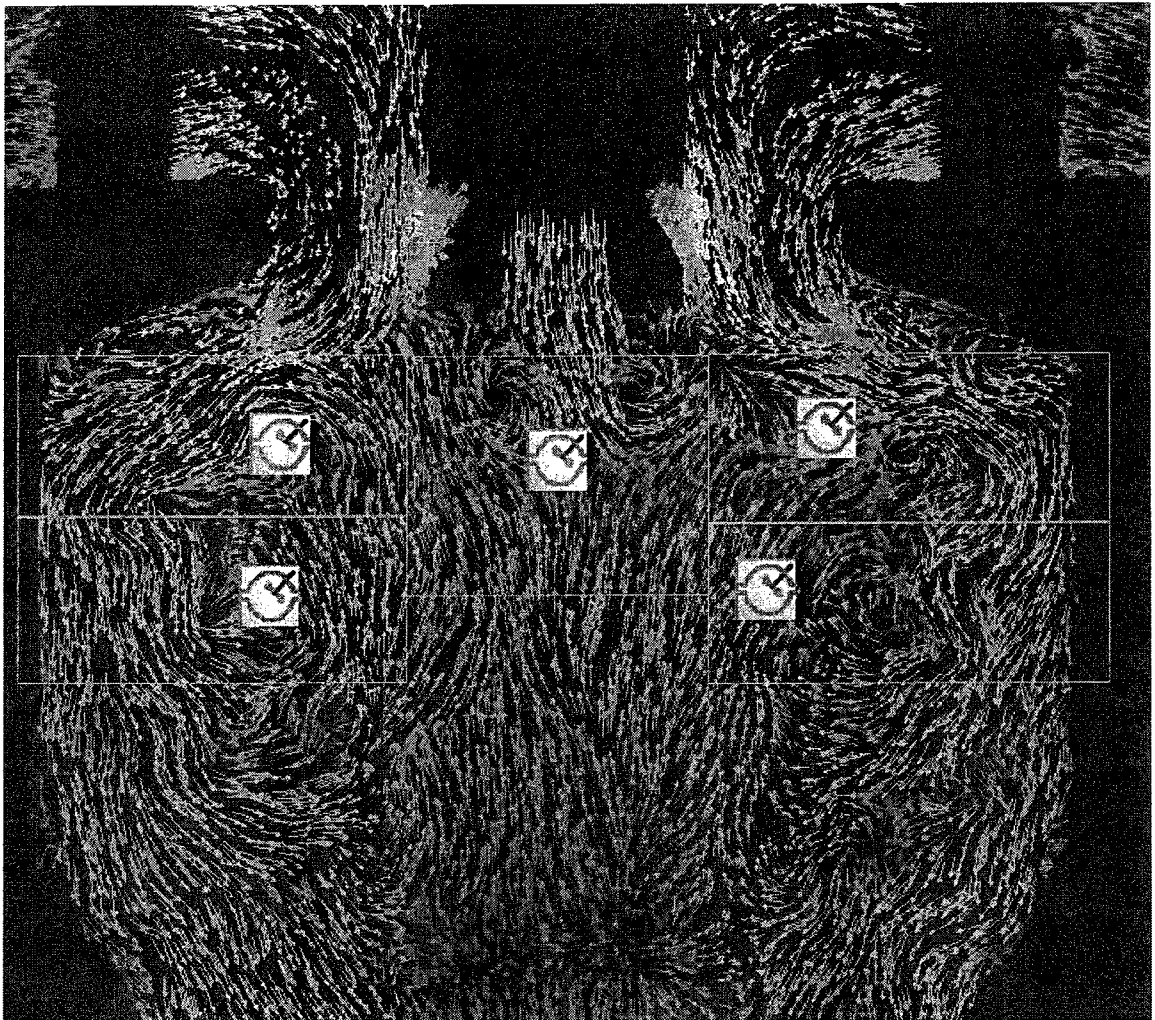


*Figure 3-1: Image of the primary zone of the combustor with virtual PSRs*

In Fig 3-1, each section represented by the red rectangle comprises of control volumes with similar properties. Each region corresponds to a perfectly stirred reactor as shown by Chemkin's PSR icons.

The reactor arrangement has traditionally been done in three different ways:



### 3.1.1 Method I

On the most basic level, for very simple 2D geometries with no recirculating flows, the streamlines are drawn and divided into several plug flow reactors. The division is refined until no considerable change is observed in the results; or in other words a sensitivity analysis is implemented via the number of reactors. The figure below is a portrayal of this approach.

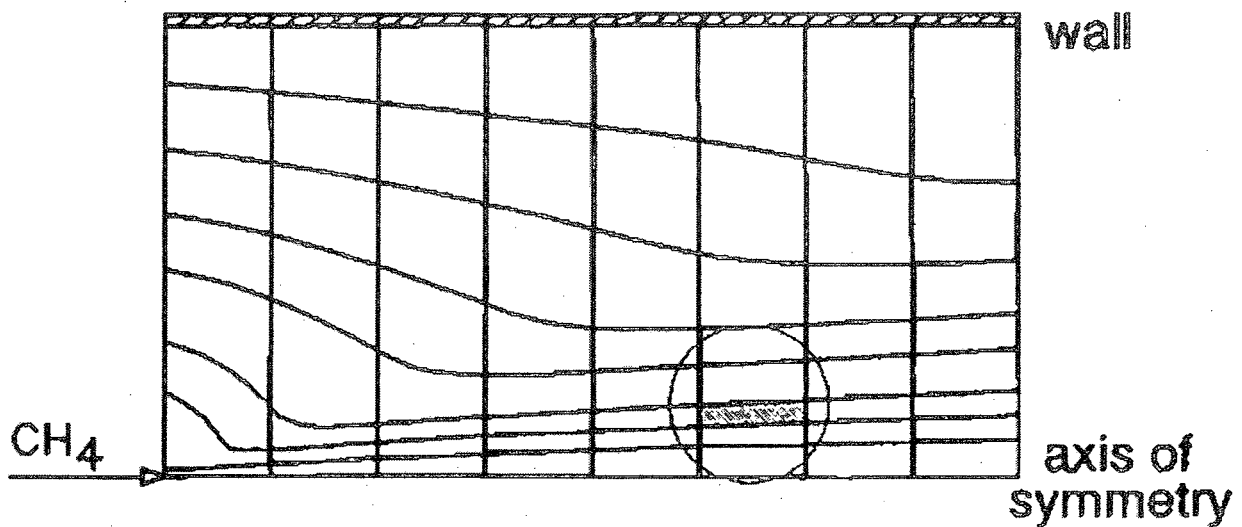


Figure 3-2: Based on the streamlines, cells are grouped to represent PFRs in series and parallel <sup>(23)</sup>

Ehrhardt et al <sup>(23)</sup> implemented a CFD analysis of a very simple 2D geometry via the k-epsilon model and chose a flow field where downstream convection is much stronger than upstream diffusion therefore simplifying the solution by solving parabolic equations. The cross sectional diffusion or mass transfer could be corrected using the eddy viscosity via the turbulent Schmidt number. A grid sensitivity analysis would then determine the right number of the plug flow reactors.

This method is straight forward to use and requires little modifications in the CRN while easing the numerical solution of the energy equation which is difficult to resolve. A grid sensitivity analysis is easy to implement since the reactors are extracted by simply coarsening the mesh by various degrees.

The over simplified geometry approach however renders this approach futile for complex geometries where a combination of recirculation zones, inlets and cooling air need to be taken into account. The flow does not act in 1D or 2D in real geometries therefore requiring a more complex approach. Implementing the equivalent 2D streamlines in large complex 3D geometries and dividing them in 3D space is immensely time consuming if not impractical.

### 3.1.2 Method II

Falcitelli et al <sup>(8)</sup> have divided the full combustor into many small perfectly stirred reactors. This solution is theoretically correct since according to Levenspiel <sup>(24)</sup> even a PFR can be represented by a number of PSRs given the number is large enough. In this method, the flow field is broken down into many small regions based on temperature and composition parameters. The grouping is done regardless of the geometrical properties and the validity of assuming a PSR behavior for each group of cells is mainly judged based on the unmixedness index in the reactor. The recycling flow (the flow that enters one reactor from another) is directly taken from the CFD calculations between the adjacent cells.

As every few cells are grouped into one reactor, the network's resolution would not be far from the CFD's resolution therefore making it easier to obtain accurate results. The resulting CRN closely resembles coarsening of the CFD mesh and running the calculations required.

For a hexahedral mesh of about 70148 nodes, which would roughly result in less than 40000 cells and for a relatively simple flow field of an opposite wall fired steam generator, over 400 reactors were needed to obtain satisfactory results <sup>(8)</sup>. This means on complex flow fields with several million cells, an unacceptable number of reactors would be required. Long calculation times could render the method less efficient than expected.

### 3.1.3 Method III

The classic method of reactor network generation is more based on skills and experience of dividing the flow field into various regions based on their velocity vectors, temperature and composition. This method has been in existence since Bragg<sup>(20)</sup> proposed the idea of representing the combustor by a PSR followed by a PFR and Swithenbank<sup>(21)</sup> suggested the use of zonal combustion modeling. It consists of dividing every section of the combustor into a few reactors. Usually a few PSRs are allocated in the primary and secondary combustor zones followed by one or two PFRs in the discharge nozzle. This is the simplest method and mainly based on an analysis of Discrete Phase Modeling results to define the reactor volumes. This method largely depends on the user's judgment therefore it may prove inefficient and time consuming for complex combustors. Andreini et al<sup>(25)</sup> have also created a reactor network based on method III.

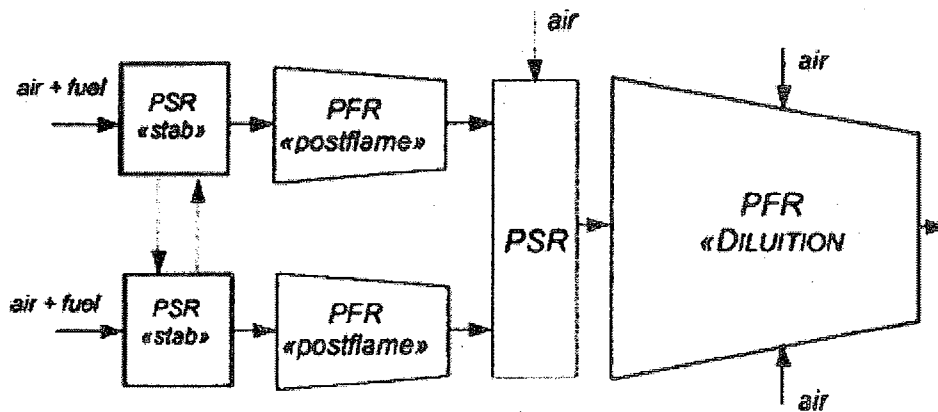


Figure 3-3: Representation of a reactor network for a LP combustor (Andreini et al<sup>(25)</sup>)

This method offers the user the ease of setting up the problem and running it within a short period of time. However, possible significant inaccuracies due to a very general representation of the flow field which is also considerably based on the user's judgment could not be justified.

### **3.2 From CFD to CRN: Current Approach**

In this work, a systematic approach is proposed. The current approach uses the best features of each traditional method while avoiding their limitations to offer a more practical way for industrial combustion analysis. An algorithm was developed to extract a CRN on an RB211 combustor. This is a DLE partially premixed combustor used on Rolls Royce's industrial RB211 engines. The method aims at initial discretization of the flow field based on its temperature and mixture fraction similar to the works of Falcitelli et al <sup>(8)</sup> and Bitondo <sup>(26)</sup>. A higher concentration of the perfectly stirred reactors (PSRs) is located in the primary and secondary zones of the combustor while the discharge nozzle area is mainly represented via one or a series of plug flow reactors (PFRs). The reactor network is refined around the flame (hot zones of the primary section) to better resolve the most influential emission regions. The fluxes are taken directly from the CFD therefore taking average mass transport between the reactors (Appendix A). This way, a systematic approach is devised using a user defined function to convey as much CFD influence as possible into the reactor network and to set up the network in the shortest possible time. Each reactor is also initialized through its species and average temperature

which are taken directly from the CFD flow field.

The logical steps for the current approach are;

- Discretization of the flow field with regards to temperature, mixture fraction and geographical location or Zone of Influence (See section 3.3 and 3.4).
- Obtaining each discretized zone's volume (see section 3.5).
- Obtaining mass flow splits between reactors (see section 3.6).
- Incorporation of the cooling air added to each reactor (see section 3.8).
- Obtain each zone's average properties such as the average temperature and mixture fraction.
- Calculation of each zone's averaged species' mole fractions. Chemkin's performance can be enhanced if an initial guess of each reactor's species mole fractions is provided. Therefore the user can average some of the main species in each reactor and provide Chemkin with the initial species' mole fractions to speed up the computational process. A reactor network initialized with flow field's averaged species can improve Chemkin's computational time up to 3 times compared with an uninitialized reactor network.

Reactor network generation has always been a difficult task since no set of firm rules have been devised regarding the degree of reactor refinement and accurate representation of inter reactor flux exchange. Also, the current chemical kinetics software package,

Chemkin, poses serious limitations on the number of inter reactor flux exchange and the type of reactors which could be linked. For example, in the main flame region where high thermal and composition gradients dominate the flow, any reactor could be exchanging mass flow with several other reactors exceeding a maximum permissible number of 10 reactor flux interconnections. Also, the higher the number of connections and the smaller the amount of mass exchanged between them, the more challenging the task of obtaining convergence would be. The current approach aims at tackling the following principal challenges;

- For accurate refinement of flow field discretization a semi automatic method needed to be devised which would ease the way for the user to generate CRNs rapidly and determine the most promising discretization parameters (ex. temperature, mixture fraction, eddy turnover time,  $\text{NO}_x$  approximation from the  $\text{NO}_x$  post processor, turbulent kinetic energy etc...)
- A method was required where the user could extract the amount of mass flow exchange between the reactors automatically.

Previously the amount of mass exchanged between reactors could not be extracted directly from the CFD simulation. The user was obliged to do the daunting task of defining simple and large reactors where the amount of mass flow rate could be roughly estimated via analytical, experimental or primitive post processing methods such as defining of iso surfaces. The author has taken advantage of an

inherent feature of Finite Volume Methods, which is the calculation of fluxes on each face, by extracting the fluxes directly from the CFD solution.

- Limitations of Chemkin had to be taken into account and only reasonable sized CRNs could be produced.
- For realistic geometries, the addition of cooling air would have serious impacts on the flow field and novel techniques would be required to take cooling air into account.
- Flexibility to deal with unstructured or some times hybrid meshes was needed.
- It was required to obtain the flexibility to run LES cases and generate CRNs within them. Since no way of accessing averaged LES results from the Fluent data file was discovered within the specified short period of time, a novel method was devised to discretize the averaged LES results in Fluent via a developed UDF. The CRN generating UDF would then discretize the field based on the user averaged LES data.

### **3.3 Mixture Fraction and Temperature**

The first step in creating a reactor network is to determine the criteria based on which the geometry would be divided into smaller sections. Based on the definitions of perfectly stirred and plug flow reactors, temperature and mixture fraction were used to divide the



flow field since they represent the thermodynamic and composition state of the flow. Falcitelli et al <sup>(8)</sup> use the stoichiometry and temperature to break down the flow field while Bitondo <sup>(26)</sup> suggests the use of temperature and mixture fraction. Mixture fraction has been used since Fluent solves the mixture fraction equation and its value is an indication of the composition of the mixture in every cell. The mixture fraction value for every cell is readily available to be accessed in Fluent and is stored by Fluent in an array. The mixture fraction is a non-dimensional variable and is defined in terms of a passive scalar that complies with the scalar transport equation without the source term.

The flow is then discretized into sections to ensure relative homogeneity in composition and thermal properties. This division is arbitrary at first, but via reactor network sensitivity analysis a final division is later selected. The idea of reactor refinement is similar to a CFD mesh sensitivity analysis. The reactor numbers are increased in regions where high thermal or composition gradients exist to ensure the flow properties in each region comply with the definition of PSRs and PFRs.

In complex geometries such as the RB211 a refined reactor network is required to represent the flow field accurately. Species such as NO<sub>x</sub> and CO are highly sensitive to temperature. Therefore the temperature gradients were specified to produce more reactors in the primary compared with the secondary and the discharge nozzle. The primary section of the combustor (see Fig 3-4) is the heart of the combustor and it has higher temperature gradients to be captured; therefore a higher number of reactors are required for this region. The high concentration of the reactors is generally applied for

temperatures exceeding 1700 K as the temperature interval that describes the homogeneity of each reactor cannot be too large. The  $\text{NO}_x$  formed via the thermal Zel'dovich mechanism increases significantly with temperatures exceeding 1700 K-1800 K<sup>(27)</sup>. Therefore care is taken to avoid averaging over large temperature intervals at high temperatures. Temperature intervals of 50 degrees and smaller are used for high temperature gradient regions in the primary section of the combustor. The variation of reactor concentration in the primary, secondary and discharge nozzle is entirely up to the user's judgment, but this variation is usually non linear.

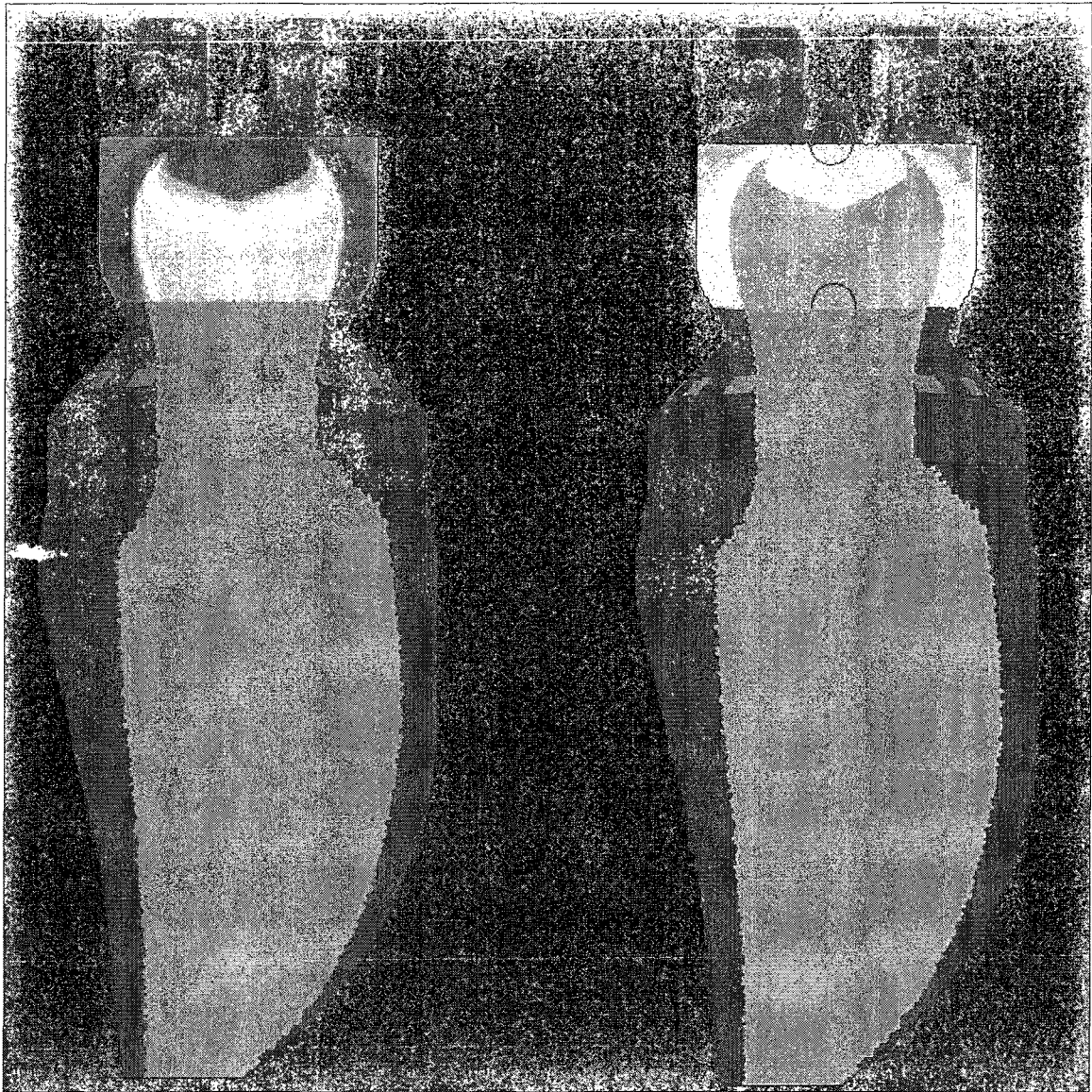


*Figure 3-4: Depiction of refined reactor resolution (left) and original resolution of reactors around the flame (right).*

Fig 3-4 is a 2D plane, cut through the RB211-DLE combustor on a RANS model <sup>(28)</sup>. The image on the right shows the division of the flow field without the refinement around the flame in the primary section. The image on the left shows the primary section with a higher concentration of reactors around the flame. Notice that the colors are arbitrary and

each one simply represents one reactor. The image on the right shows 1 reactor representing the entire flame region while the image on the left divides the flame into 3 reactors. The higher concentration of reactors ensures better uniformity of the flow properties within the reactor. The two circles on the left image indicate the clear cut lines which are the boundaries separating the primary, the secondary and the pre-mixer as a consequence of the Zone of Influence criteria (see section 3.4).

### **3.4 Zone of Influence**

In order to avoid grouping of the distant cells which fall into the same mixture fraction and temperature category, a numerical construct so-called ‘the Zone of Influence (ZoI)’ traverses the flow field (by looping through every  $x, y, z$  value of the domain), creating reactors according to the thermal and mixture fraction filtering criteria. ZoI (simply the delta  $x, y, z$  in three-dimensional space) can be used in order to control the number of reactors being formed. For example, a greater delta  $x$  value will create fewer reactors within an interval of  $x$ . In this manner, the ‘zone’ moves throughout the combustor region, creating reactors as it passes through. Therefore, the concept of ZoI is mainly used by the author to distinguish every stage of the combustor which are the primary, the secondary and the discharge nozzle and to avoid any insignificant pieces such as the fuel bars to be discretized into reactors. This is because the ideal reactor formulations are only

valid for the bulk flow and not for flows close to walls where boundary layers influence the flow field <sup>(9)</sup>.

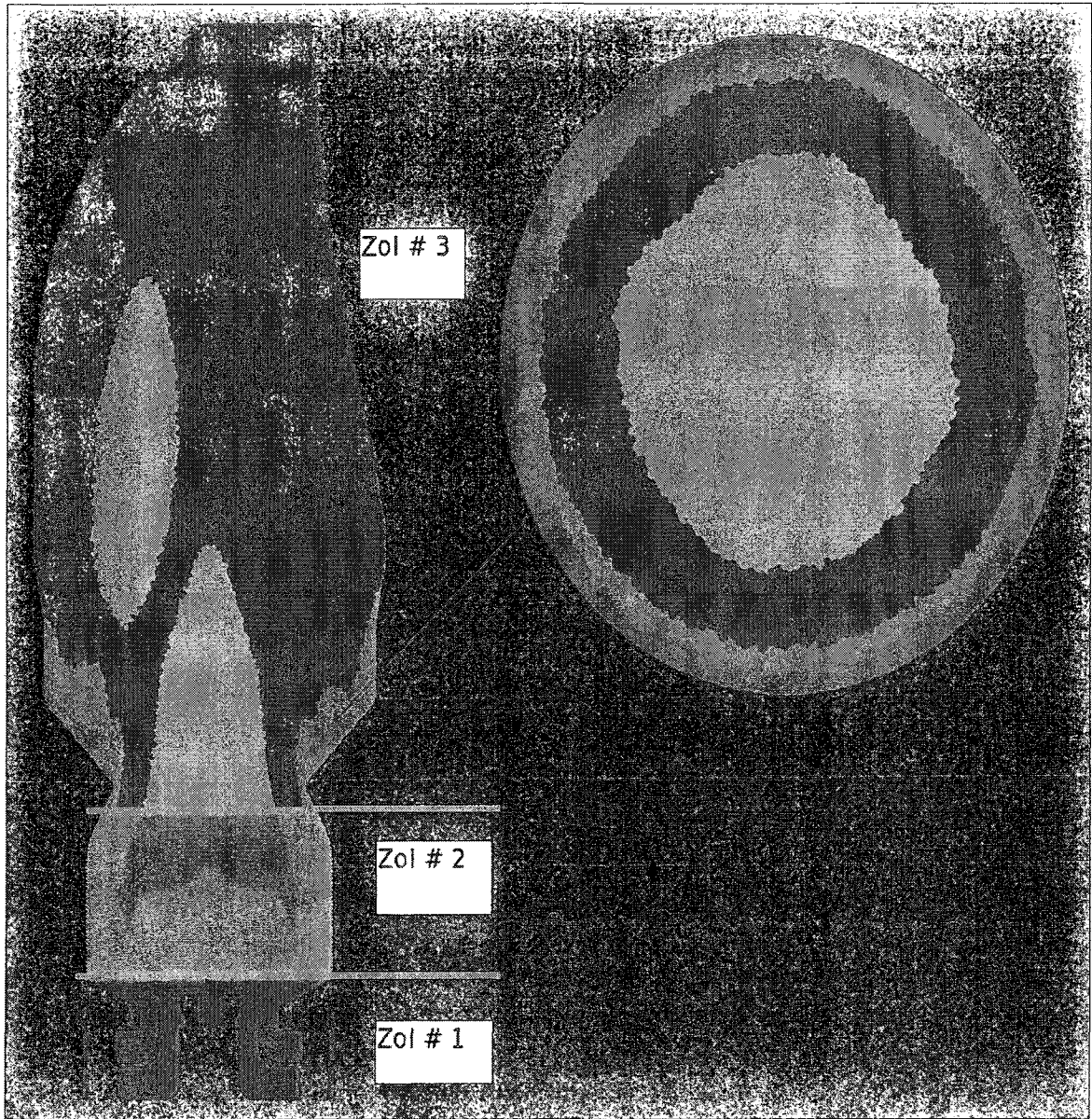


*Figure 3-5: A sample of the flow field discretization within each Zol on a RB211 RANS model.*

In Fig 3-5, the colors are random and each represents one reactor. It is noticed that the boundaries indicated by the purple lines divide the flow field geometrically first before

the reactor extraction based on temperature and composition occurs within each zone (ZoI). The circular figure on the right is a cross sectional cut of the geometry where the arrow points at. There is a clear division of the cells as they move further away from the walls. Since ZoI works on the entire domain, it is useful to construct the grid as consisting of two or three fluid domains (primary, secondary, discharge nozzle) in order to constrain the ZoI to work on specific regions and to visualize them.

### **3.5 Volume and Residence Time**

The issues regarding the residence time and reactor generation were an exhausting and challenging part of this project. Almost in all of the available literature, the calculation of the recycling flows has not been explained in detail and the residence time calculation has been done in different ways. For example, Bitondo <sup>(26)</sup> has made an attempt at using the classic particle tracking method for residence time estimation. Although major problems (such as--proprietary info--) prevented him from obtaining a reasonable reactor network, his techniques are acceptable and useful. Rubins and Pratt <sup>(29)</sup> carried out a water tunnel test to become familiar with the flow field in their ALF-502 GT combustor before generating their reactor network.

Traditionally the residence time has been obtained via particle tracking and steady or pulse tracer methods. These options have been examined and used by researchers such as Pedersen et al <sup>(30)</sup> and Bitondo <sup>(26)</sup>.

The current method is based on accessing the cells and summing of their volumes and masses. Chemkin calculates the residence time based on each reactor's net mass flow rate and volume. Therefore, the simplest method is to provide Chemkin with reactor volumes directly taken from the CFD flow field. The current approach is based on the works of Mohamed<sup>(31)</sup> and Novosselov<sup>(32)</sup> and is used by Chemkin<sup>(12)</sup>. The mass of each reactor is calculated by the addition of the mass of every composing cell and the total reactor mass is divided by the mass flow rate to obtain an average residence time which is directly fed into Chemkin (Equations 3.1-3.2).

Although Discrete Phase Modeling was tried for the RB211 combustor<sup>(33)</sup>, it has been rejected as a reliable method due to its complexity and time consumption for complex reactor networks. Moreover, automatic creation of complex iso-surfaces is not possible in Fluent and the task of iso-clipping surfaces, which define PSR zones, according to the filtering criteria is not a practical option. CRN Generation is thus needed to be semi-automatic at least and considerable programming has been required to ease this problem.

The residence time can be calculated as follows;

$$\tau_R = \frac{\rho V}{\dot{m}}$$

*Equation 3.1*

Or

$$\tau_R = \frac{V}{\dot{V}}$$

*Equation 3.2*

### **3.6 Flow Mass Split**

Chemkin requires the flow mass split to be defined as the percentage of exit mass flow rate. The sum of the exit reactor mass flow fractions must equal 1 up to 6 decimal digits. Due to the high accuracy required in Chemkin regarding the specification of the recycling mass flow fractions, it is therefore suggested to use the double precision “3ddp” version of Fluent. The mass flow splits may not always be equal to 1 up to 6 decimal digits in the single precision “3d” version of Fluent due to the round off errors. While care is taken to isolate and regroup such reactors, it is necessary to avoid round off errors.

The mass flow splits are extracted between each two adjacent reactors. When two reactors neighbor, the flow density, the flow velocity and the area at their interface are taken to calculate the mass flow rate between them. Finally, all the mass flow rates between the neighboring cells are added up to obtain the total mass flow exchange with the surrounding reactors. The steps for obtaining mass flow split for each reactor are;



1. First the total mass flow rate through reactor  $R_i$  is calculated.

$$\dot{m}_{R_i, total} = \sum_1^{N_{R_i}} (\rho_{c, R_i} \times A_{f, c, R_i} \times v_{f, c, R_i})$$

*Equation 3.3*

2. Then the mass flow rate from reactor  $R_i$  into  $R_j$  is calculated and divided by the total mass flow rate through reactor  $R_i$  to produce the recycling fraction ratio from  $R_i$  to  $R_j$ . This value is required by Chemkin.

$$\dot{m}_{R_i, R_j} = \frac{\sum_1^{N_{R_i, R_j}} (\rho_{c, R_i} \times A_{f, c, R_i} \times v_{f, c, R_i, R_j})}{\dot{m}_{R_i, total}}$$

*Equation 3.4*

- $\dot{m}_{R_i, R_j}$  is the mass flow rate from  $R_i$  into  $R_j$
- $\dot{m}_{R_i, total}$  is the total mass flow rate through Reactor  $R_i$
- $\rho_{c, R_i}$  is the density at cell “c” of reactor  $R_i$  which is a boundary cell
- $A_{f, c, R_i}$  is the area of face “f” of reactor  $R_i$  which is a boundary face belonging to cell “c”
- $v_{f, c, R_i}$  is the velocity at the boundary face “f” in reactor  $R_i$  which belongs to cell “c”
- $v_{f, c, R_i, R_j}$  is the velocity vector from Reactor  $R_i$  into Reactor  $R_j$  at face “f” of cell “c”

- $N_{R_i}$  is the maximum number of faces (belonging to cell “c”) which comprise the boundaries of Reactor  $R_i$
- $N_{R_i, R_j}$  is the maximum number of boundary faces shared by Reactors  $R_i$  and  $R_j$

### 3.7 Removal of Small Reactor

On complex geometries with millions of cells such as the case of the RB211, there are cells which may form small reactors due to unphysical characteristics originating from the numerical or mesh quality inaccuracies or simply due to the division intervals used. These small groups of cells can hinder the reactor network analysis in two ways:

1. Creation of negligibly small recycling mass flows sometimes causes the reactor recycling interconnections to exceed the allowable limit which is 10 recycling connections for PSRs.
2. Convergence difficulties in Chemkin due to small residence times in these reactors

From experience, the residence times in these reactors are extremely small and the number of cells in them may be less than 300 in a mesh containing millions of cells. In a

CFD field with millions of cells, it would be practical to remove these reactors and avoid all the numerical and software difficulties associated with them. (Appendix B).

### **3.8 Addition of Cooling Air via Source Terms**

In the CFD simulations of the RB211-DLE combustor, it was realized that the use of source terms for the effusion cooling air were much more preferable to converting walls into mass flow inlets to introduce cooling air. The use of source terms proved to achieve more realistic CFD temperature fields. However, since these source terms are not available with regular identification names (thread ID, cell ID, inlet boundary ID etc...), the problem of introducing their existence into the CRN needed to be solved. The following technique was devised to incorporate their effect into the reactor network.

- Mark the layer of cells adjacent to the walls in the primary, the secondary and the discharge nozzle of the combustor separately in order for Fluent to assign each one a unique thread ID <sup>(34)</sup>. The author identifies each thread by naming them flux-primary, flux-secondary and flux-discharge nozzle.
- Apply the source terms uniformly across the marked zones in each stage of the combustor
- For each reactor that includes cells from one of the flux-primary, flux-secondary

or flux-discharge nozzle, calculate the volume of cells and multiply them by the source term mass flow constant. The contribution of source terms due to each one of these flux zones is then reported to the user.

The source term effects can be incorporated into the reactor network via the extra inlets attached to the source term containing reactors. This approach was validated and presented in the technical communication <sup>(35)</sup>.

$$\dot{m}_{j,Source} = \left( \left( \sum_1^N V_i \right) \times C_{s,primary} \right)_{primary} + \left( \left( \sum_1^N V_i \right) \times C_{s,secondary} \right)_{secondary} + \left( \left( \sum_1^N V_i \right) \times C_{s,discharge-nozzle} \right)_{discharge-nozzle}$$

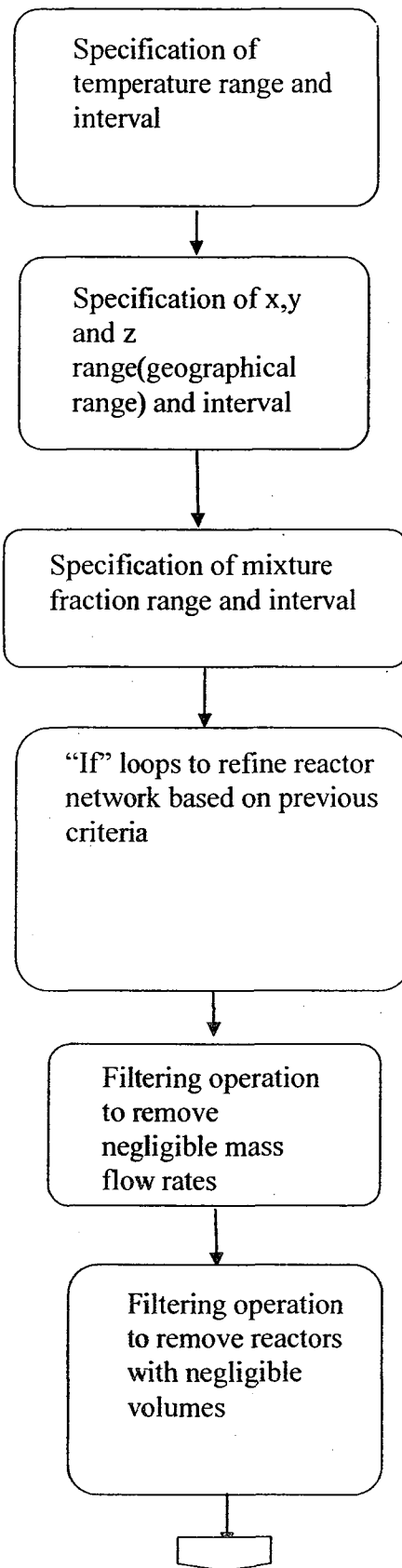
*Equation 3.5*

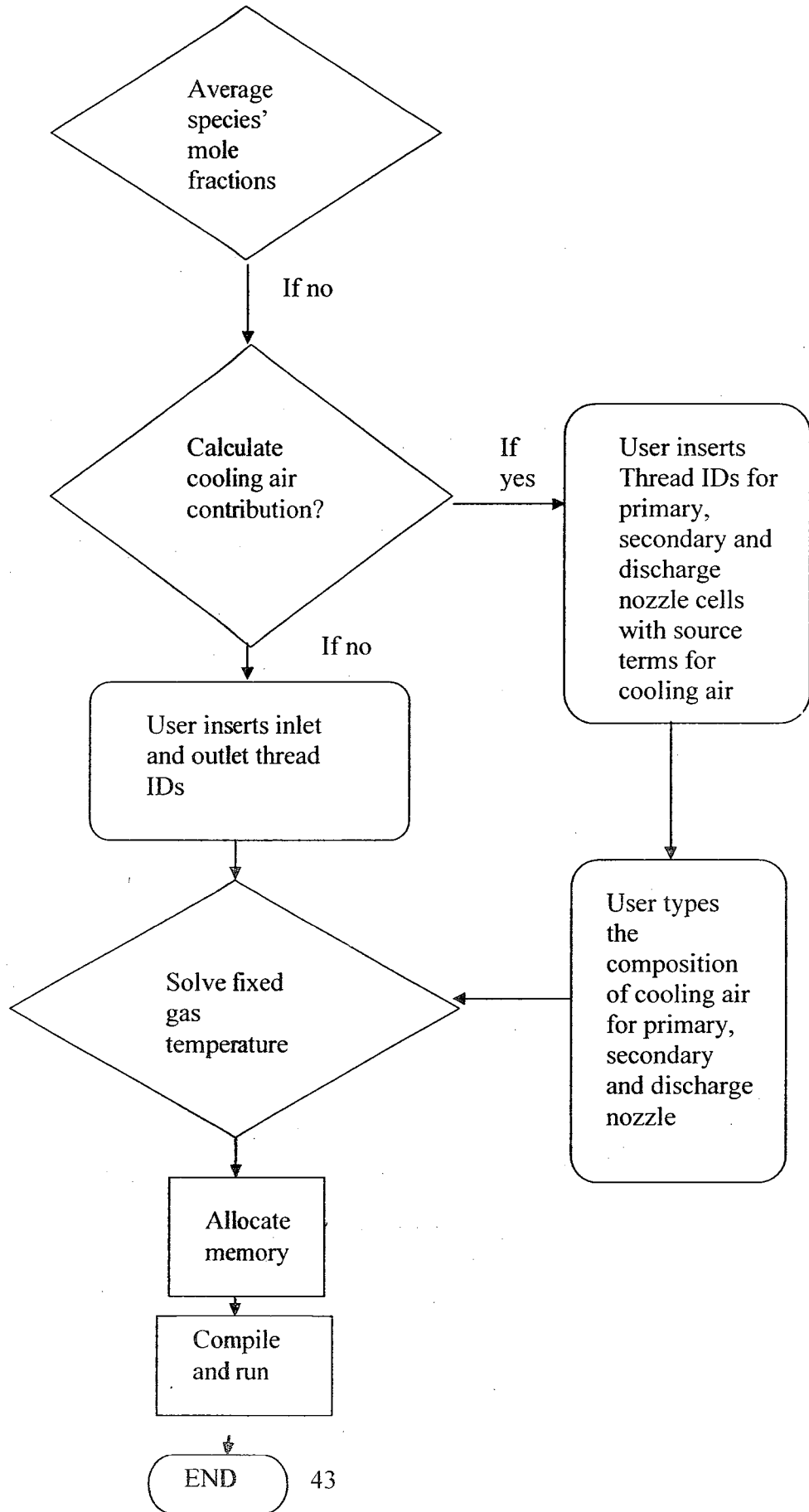
where;

- “*i*” is the cell number
- *V* is the cell volume
- “*N*” is the maximum number of cells which contain source terms
- *C<sub>s</sub>* is the source term mass flow constant
- $\dot{m}_{j,Source}$  is the mass flow rate due to source terms in reactor *j*

### 3.9 CFD-CRN Generation Algorithm Flow Chart

Once a well validated CFD simulation is in hand, a set of standard steps need to be taken for the creation of reactor networks. The following flow chart describes a summary of these steps.





## 4 ALGORITHM APPLICATIONS

It was soon found out that manual post processing of the CFD simulations with millions of cells for the discretization and generation of CRNs would be extremely time consuming if not impractical. The need for a semi automated robust way of discretizing the flow field based on various parameters for sensitivity analysis encouraged the development of a program in the form of a User Defined Function or UDF. The limitations of Fluent, lack of available information and initial unreasonably slow speed of the UDF posed difficulties in coding of the algorithm.

An initial success in the coding of the CRN generating algorithm (in the form of a User Defined Function) was achieved via the extensive use of the data structures which at the same time proved to be too slow to be considered highly efficient. The running of about 20,000 cells would take over 20 minutes and over an hour for 60,000 cells. The flow field was successfully divided into various regions and the recycling flows and the temperature fields were averaged.

Several attempts at restructuring the coding mechanism were made in order to improve speed. The current use of look up tables and reducing the use of link lists has proven to



guarantee efficiency and high speed. The current division of the field based on various parameters and without initializing the species for every reactor takes about 5 minutes for 3 million cells which is an astounding enhancement compared to the initial versions of the UDF.

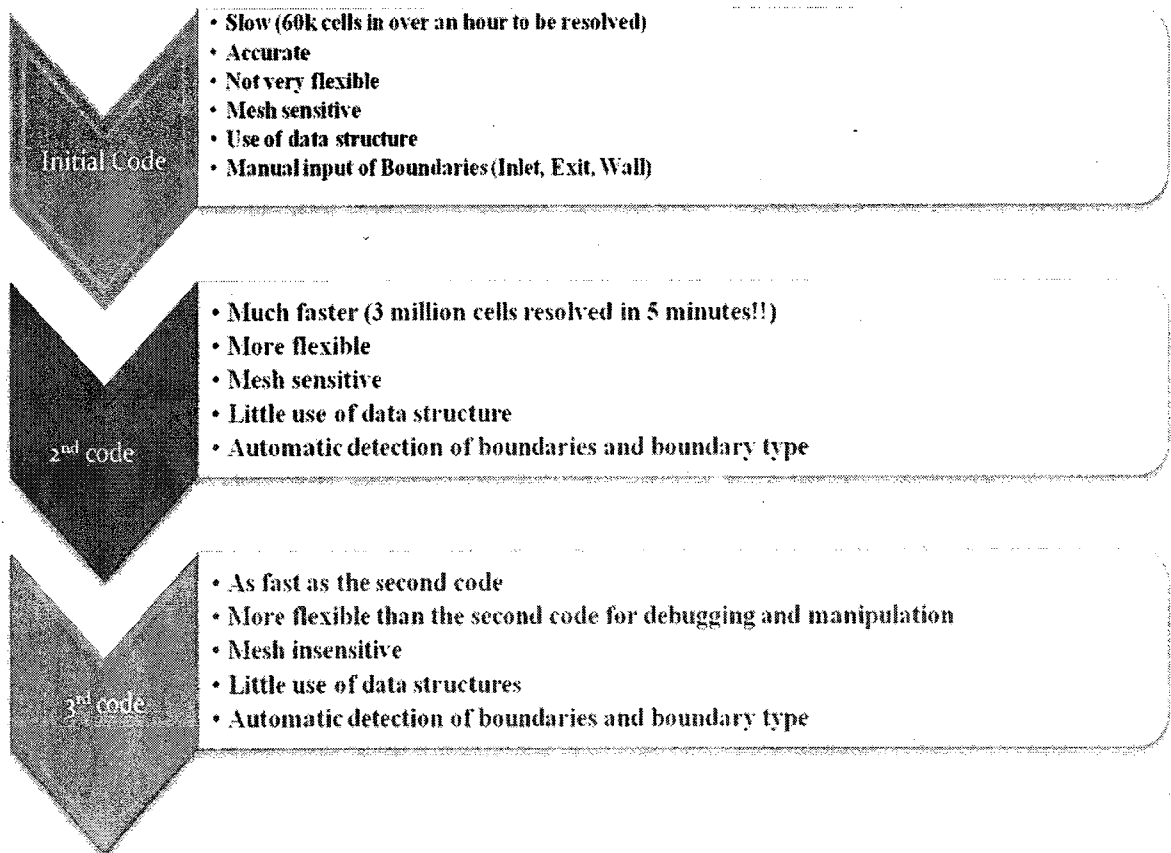


*Figure 4-1 A representation of the programming phases of the developed algorithm for RB211 analysis*

Chemkin imposes limits on the number of connections each reactor can have. For PSRs a maximum of 10 recycling connections can be specified. Occasionally a reactor might neighbor a few other reactors where it feeds and receives mass flow with each one therefore exceeding a maximum of 10 connections.

It happens very often that some of these recycling ratios are negligibly small and therefore the user can define a cut off recycling ratio threshold under which all mass flow recycling fractions are removed and their mass flow rate is evenly distributed among the other neighboring reactors. This method conserves mass while avoiding small recycling ratios which cause modeling difficulties in Chemkin.

#### 4.1 CFD Simulation of an RB211 Combustor

Initially, a RANS simulation of the RB211 was implemented via a polyhedral mesh to reduce the cell count and speed up the reactor network generation. The CRN generating algorithm was developed with respect to this model and later was utilized on averaged LES models for the cases mentioned before. The  $k-\varepsilon$  realizable model was used with a standard wall function. Mr.Sandeep Jella compared the CFD with the validated geometry presented for his MASc<sup>(28)</sup> and confirmed the validity of the flow field. The geometry consisted of 3379137 cells, 21558796 faces and 17831079 nodes. The cooling air is simulated via the source terms in the layer of cells adjacent to the walls separately

for primary zone, secondary zone and the discharge nozzle.

Fig 4-2 to 4-5 show the type of flow field, geometry and the grid initially used for the development of *CRN Generator* (the CRN generating algorithm). The algorithm was successfully run for hexahedral, tetrahedral and polyhedral meshes on preliminary cases.

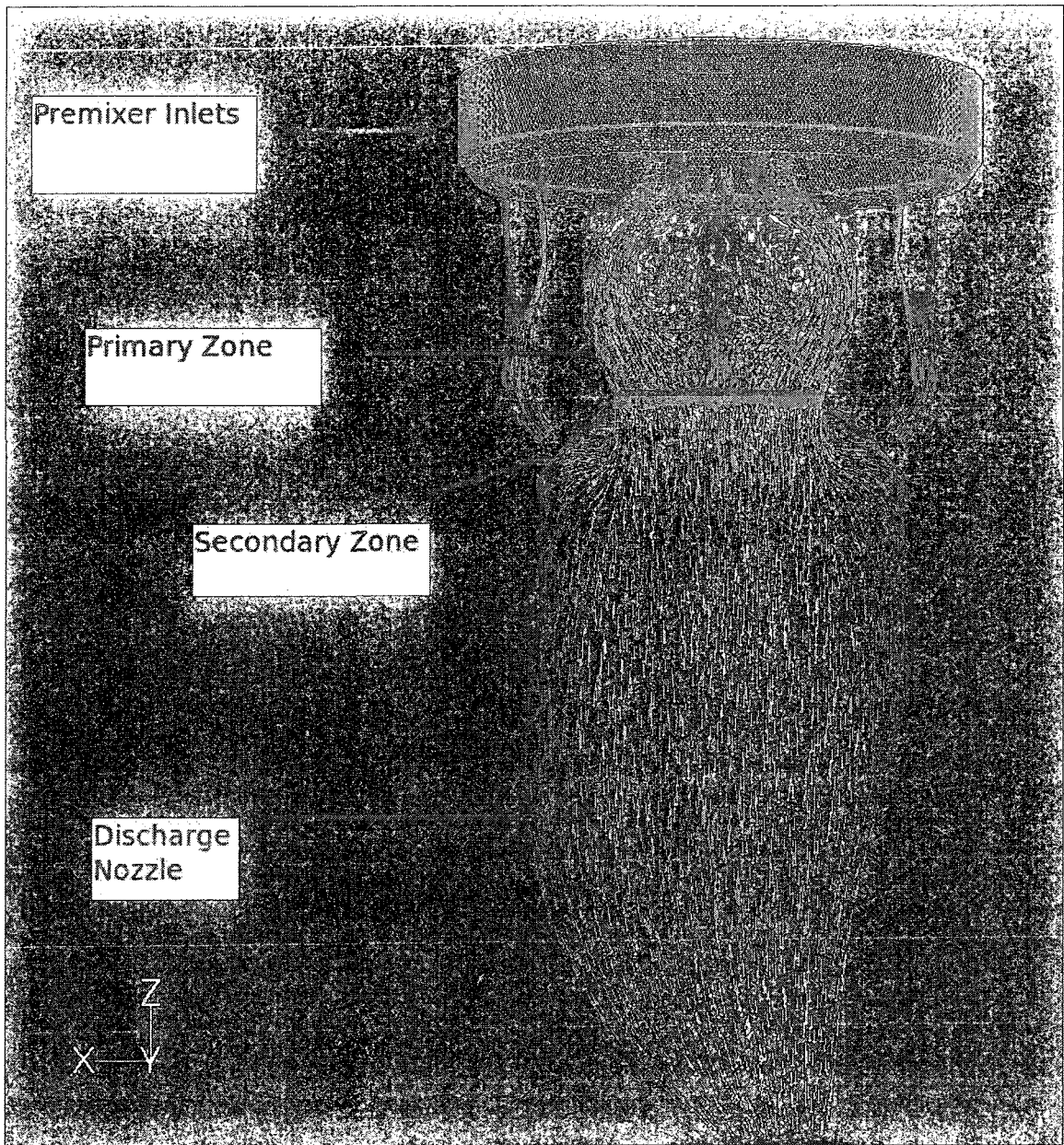
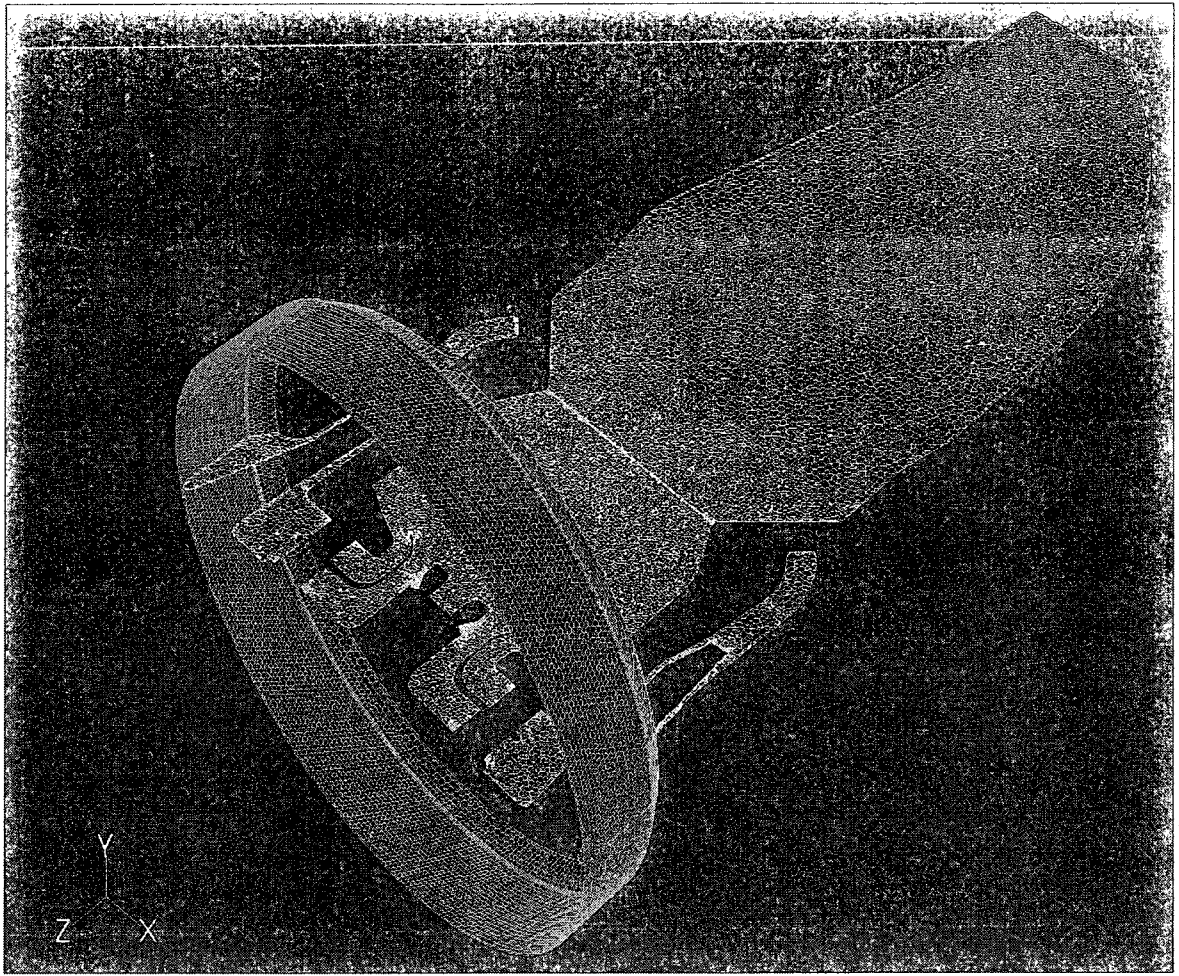


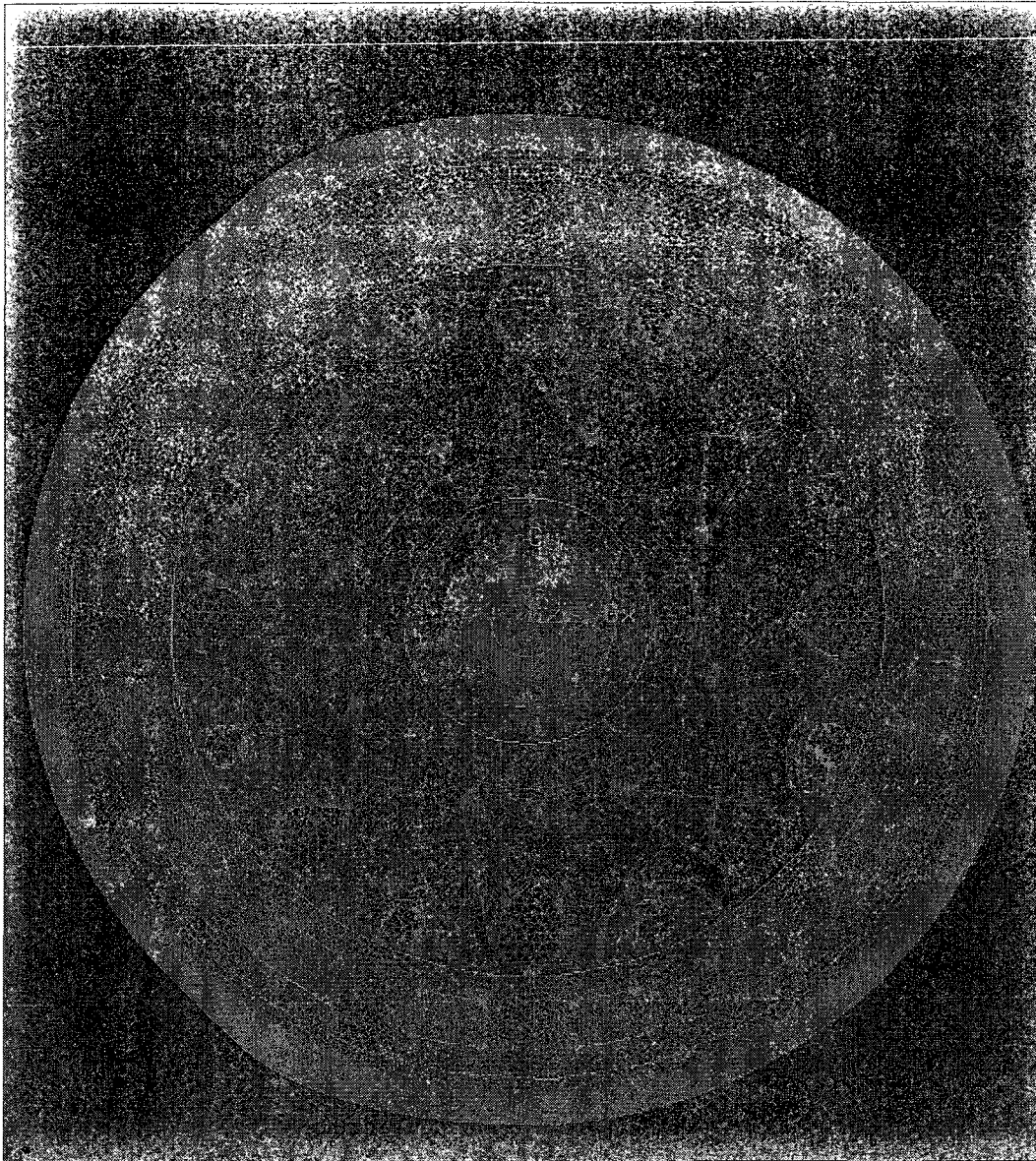
Figure 4-2: 2D portrayal of velocity vectors and the premixer grid



*Figure 4-3: Sample of the mesh used*



*Figure 4-4: 3D complex mesh on RB211*



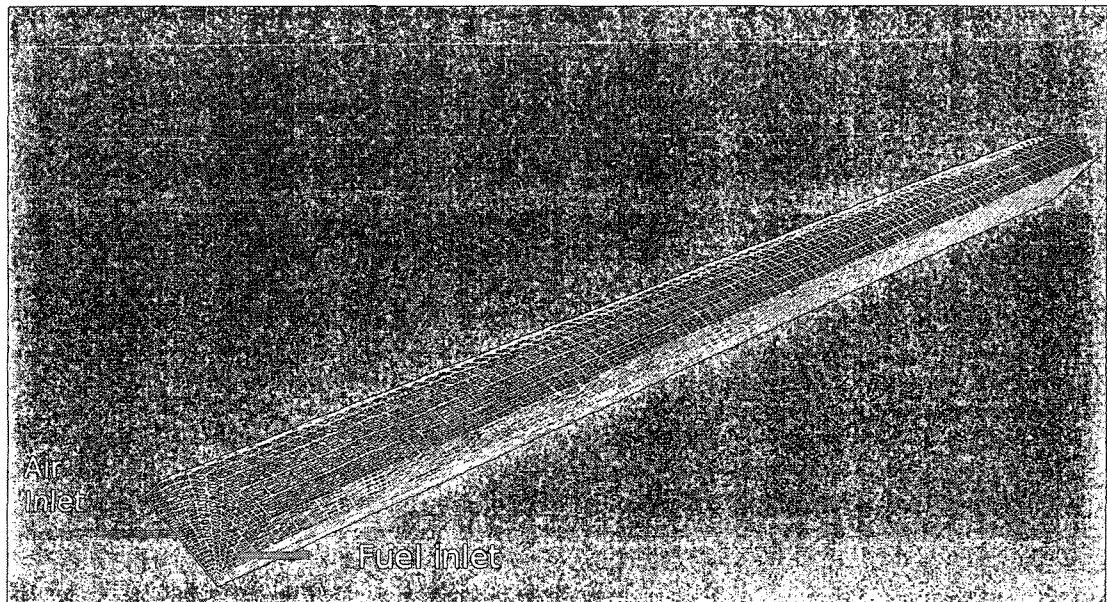
*Figure 4-5: Premixer and secondary windows' mesh*

Fig 4-3 is a cut through the geometry showing the unstructured grid. As observed there is a higher concentration of mesh points in the primary section of the combustor due to high gradients and detail turbulence-combustion effects. The premixer region is not of concern to chemical reactor network generation since no reaction occurs. Ideal reactors are also

not capable of dealing with boundary layers and strain rate effects which dominate the premixer flow; therefore their use is mainly limited to the bulk flow.

## 4.2 CFD Simulation of Simpler Models

The CFD and CRN simulations were initially started on a simple academic combustor<sup>(37)</sup>. The Lockwood combustor was believed to be a reasonable case to tackle even though the higher temperature and composition gradients, as a result of being a diffusion flame, are generally not favorable in forming CRNs. The CFD simulation was well validated based on the mixture fraction and velocity data.



*Figure 4-6: Lockwood geometry*



Later, a 45 degree slice of the primary section of the RB211 combustor was also analyzed and the CFD results were compared with Ref 36. The flow field was in reasonable correspondence with the experimental data except for a very small patch of higher temperature region which was also unexplained by the experimental data.

Fig 4-7 is a depiction of the temperature contour in the 45 degree slice of the primary section of the combustor.

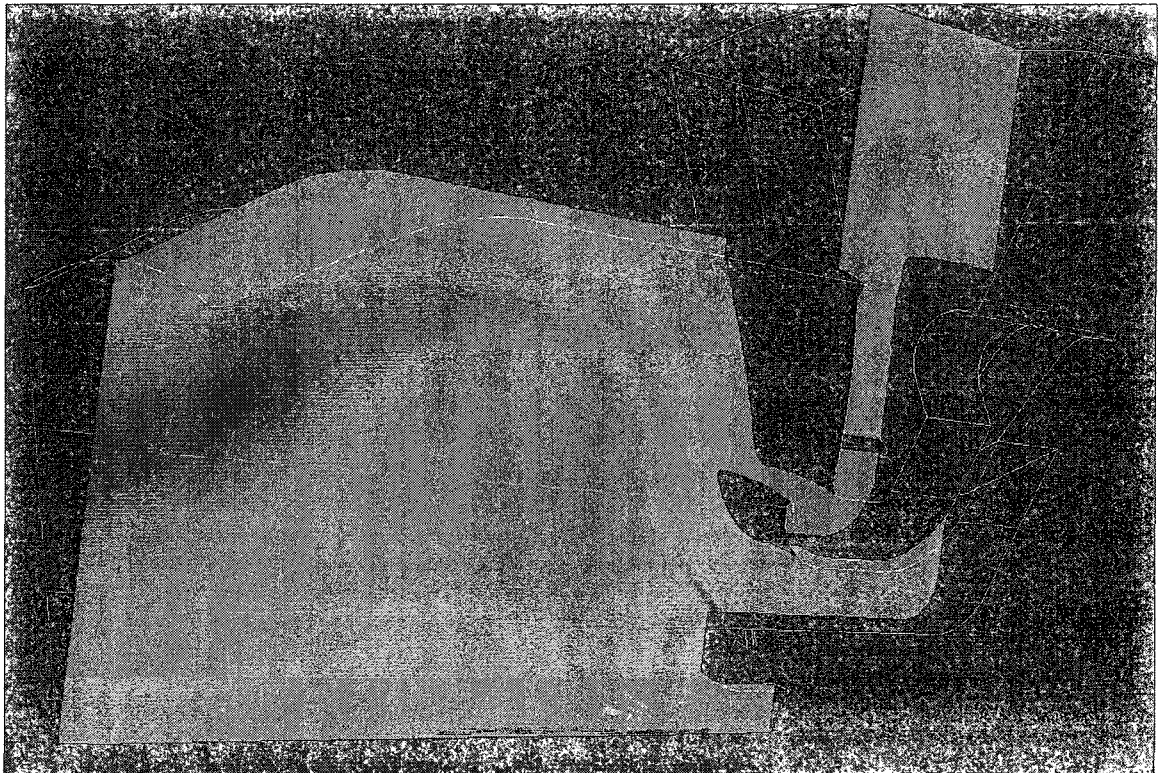


*Figure 4-7: RB211 combustor 45 degree slice*

## **4.3 Reactor Generation**

The current method aims at automatic generation of a ready to use input file for use in Chemkin which describes the PSR arrangement and their recycling ratios. Chemkin provides the capability of defining each type of reactor (PSR, PFR etc ...) via an input file. This feature is an inherent characteristic from its original source code, but the capability of integrating different types of reactors is not available via the input file. For example, a PSR connected to a PFR can not be generated via an input file. Chemkin provides this capability only via the graphical user interface. Therefore the current approach is to generate a network of PSRs and manually attach any non PSR reactors via the graphical user interface.

The input file generated is directly read into Chemkin and is made up of 4 principal sections which describe the number of reactors, reactor arrangement, reactor properties and cooling air inlets from source terms (if available).

### **4.3.1 Description of Input File**

The input file includes commands which instruct Chemkin to use a steady state or transient solver, to solve the energy equation or assume fixed temperatures. This part also informs Chemkin of the number of reactors in the network. Failure to have the exact

number of reactors inserted into the input file will prevent Chemkin from reading the input file. The “!” sign is used to add comments in Chemkin.

```
|-----|
```

```
! CRN 2007-2008
```

```
! By Sam G. Hesami
```

```
! In collaboration with Rolls Royce Canada and Concordia University
```

```
|-----|
```

*Figure 4-8: Input file heading*

```
NPSR 17 ! Number of Reactors After Reactor Re-arrangement and Downsizing
```

```
STST ! Instructs Chemkin to Use a Steady State Solver
```

```
TGIV ! Instructs Chemkin to Use Fixed Gas Temperature
```

*Figure 4-9: Input file part I*

Section I of the input file to Chemkin includes the headings and defines the number of reactors and the type of solver. Fig 4-9 is part of the input file generated which specifies the number of reactors, the solver type and the status regarding the solution of the energy equation.

Part II of the input file includes the information regarding the mass flow splits. Each line starts with RECY which stands for “recycle” followed by the donor and the receiver reactor IDs respectively. For example, in the 1<sup>st</sup> line of Fig 4-10, 1.007885157 % of the mass flow through reactor 17 recycles into reactor 4.

LINE 1) RECY 17	4	0.01007885157	! Reactor 17 feeds reactor 4
LINE 2) RECY 17	5	0.02287825415	! Reactor 17 feeds reactor 5
LINE 3) RECY 17	6	0.00987549046	! Reactor 17 feeds reactor 6
LINE 4) RECY 2	3	0.9728576482	! Reactor 2 feeds reactor 3
LINE 5) RECY 2	4	0.01820507898	! Reactor 2 feeds reactor 4
LINE 6) RECY 2	1	0.008937272792	! Reactor 2 feeds reactor 1
LINE 7) RECY 3	17	0.0156725567	! Reactor 3 feeds reactor 17
LINE 8) RECY 3	2	0.2984216001	! Reactor 3 feeds reactor 2
LINE 9) RECY 3	4	0.6859058432	! Reactor 3 feeds reactor 4

*Figure 4-10: Input file part II*

Part III of the input file contains information about each reactor’s volume, pressure, temperature and the average species (optional). The following sample has been taken from an input file. The number “17” in bold refers to the reactor number for which the conditions are defined. The underlined values correspond to the quantity of pressure, temperature, volume and species mole fractions.

!Surface\_Temperature 1 !Surface Temperature Same as Gas Temperature

PRES	<u>3</u>	17	!Pressure (atmospheres)
TEMP	<u>1292.58</u>	17	!Temperature (Kelvins)
VOL	<u>5153.88</u>	17	!Volume(cm^3)
XEST H2	<u>1.76194e-06</u>		!Mole fraction
XEST H	<u>4.54261e-08</u>		!Mole fraction
XEST O	<u>6.72712e-06</u>		!Mole fraction
XEST O2	<u>0.147503</u>		!Mole fraction

*Figure 4-11: Input file part III*

In part IV, the inlets to the reactor network are defined. The physical boundary inlets need to be defined manually via the GUI, but the source terms appear automatically as mass flow inlets in the input file. These mass flow inlets are defined via their mass flow rate, temperature and the reactors they feed. The following sample is from an automatically generated input file which defines the inlet streams to the reactor. The number 10 in bold in the first line defines which reactor the stream feeds and the following lines define the inlet stream's temperature, composition and mass flow rate.

```

INLET      Syflux      10      ! Inlet Stream-> defines which reactor it feeds

TINL      Syflux      702      ! Inlet Temperature (K)

REAC      Syflux N2    0.78991 ! Reactant Fraction (mole fraction)

REAC      Syflux O2    0.21008 ! Reactant Fraction (mole fraction)

REAC      Syflux CH4   0        ! Reactant Fraction (mole fraction)

FLRT      Syflux      3.24187 ! Mass Flow Rate (g/sec)

```

*Figure 4-12: Input file part IV*

An experienced user can change these parameters in any text editor in Windows or Linux.

### **4.3.2 Graphical Display**

The reactors within the CFD field are referred to in Fluent by their ID numbers. The reactor number each cell belongs to is stored in the cell via the User Defined Memory <sup>(34)</sup>. The reactor configuration can be visualized in Fluent via the Contour option.



*Figure 4-13: Eleven 3D reactors displayed on Fluent GUI*

In Fig 4-13 and Fig 5-6 the reactors represent the entire RB211 combustor and each color on the CFD field corresponds to the reactor number it represents. This method allows the user to visualize the generated reactor network within Fluent itself, and helps in identifying each reactor's location for post processing purposes.

## 4.4 Reactor Networks in Chemkin

The current method groups and processes the cells available and generates a complex reactor network where the temperature and species' mole fractions have been averaged over each reactor. It then generates an input file which could be directly read into Chemkin for further analysis (see section 4.3.1). At the first glance the reactors appear as a simple group of reactors connected in a row as shown below.



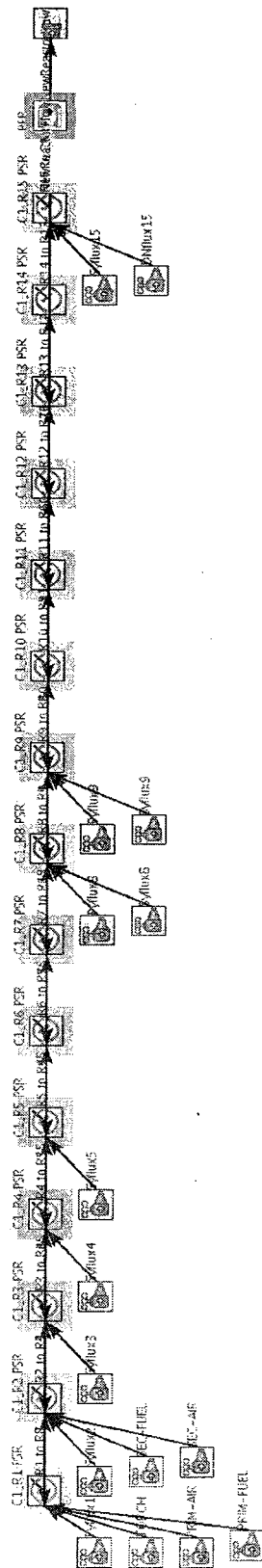


Figure 4-14: Initial view of CRN in Chemkin's GUI

However by expanding the reactor network the complexity of the connections can be revealed as depicted in Fig 4-15.

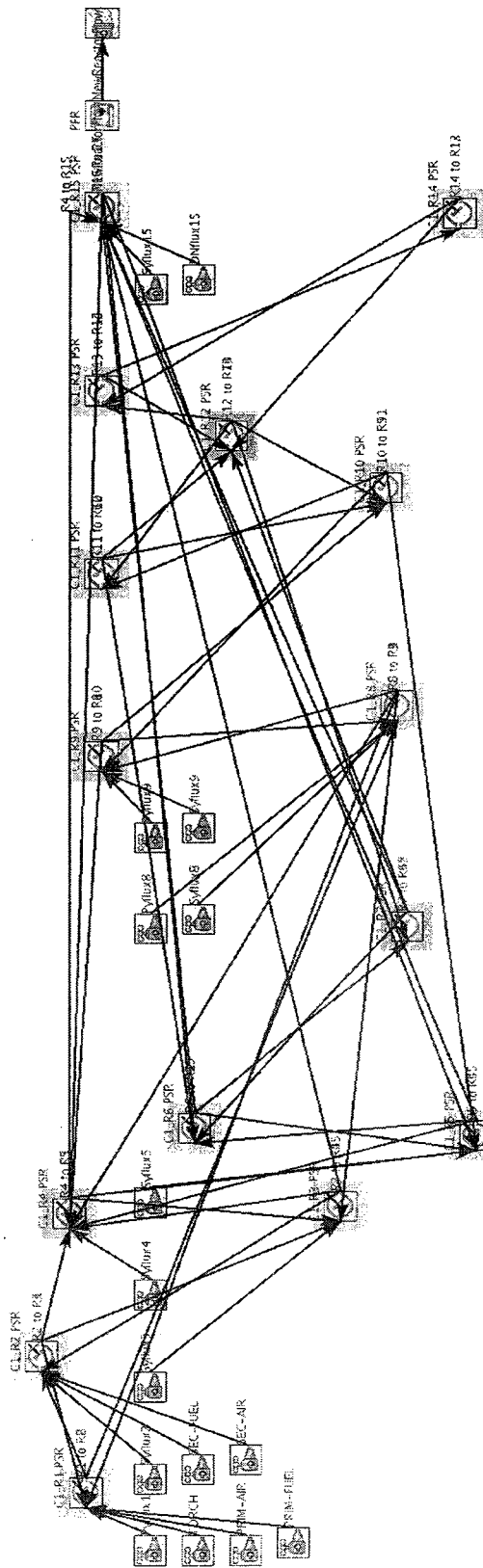


Figure 4-15: Expanded view of CRN on Chemkin's GUI

The user can find more information about each reactor in the network on the screen in its expanded version. Since the premixer does not play a role in the reactor network analysis, the recycling flows into the premixer section of the combustor (which are very small and due to flow discretization) are manually set to zero. The reactor network appears as a tree on the left side of Chemkin's graphical interface and the Chemkin post processor allows the user to view the calculated properties in each reactor. The user can select each reactor or its recycling connections for further information or modification. The user can also verify the properties of the reactor network by implementing a contour of the flow field properties in Fluent under the "Display" option. Convergence in Chemkin is a difficult task for complex reactor networks. There is no hard rule for numerical stability and better convergence can only be obtained via more advanced solvers. Incorporation of more advanced solvers in Chemkin is up to Reaction Design and is not within the user's ability to modify the solver in Chemkin. However utilization of smaller number of reactors would enhance convergence.

The flow connections in the central reactors in Fig 4-15 represent the cooling air which have been extracted and connected to their corresponding reactors. The cooling air has been represented as source terms adjacent to the walls in the CFD simulations.

## 4.5 Summary

A review has been done of the challenges posed by the complicated geometry, CFD solution and coupling of CFD-CRN. A method and an algorithm were developed in order to discretize the CFD flow field and generate an *input file* containing all the CRN information. This input file could later be read into Chemkin with minimum user interaction. The cooling air would also be taken into account via source terms allocated adjacent next to the walls. The source terms would be automatically picked up and their mass flow rate would be reported into the input file. The automatic generation of an input file would turn hours of CRN generation into minutes and therefore enhancing any sensitivity analyses required.

The reactors could also be displayed on Fluent via its contour option. The reactors would be displayed based on their allocated ID numbers; however the colors assigned to them are arbitrary. Reactor visualization would allow the author to analyze and troubleshoot the state of the reactors for any further adjustments.

## 5 RESULTS

A series of geometries were examined starting from the simplest one (see section 5.1) to a very complex RB211 combustor (see section 5.3). The simpler geometries were used in order to troubleshoot the methodology and the algorithm before taking over more difficult tasks. The results illustrates the robustness and efficiency of the present algorithm developed.

### 5.1 CRN Simulation of the Lockwood Combustor

Lockwood did not conduct emissions measurements on his combustor <sup>(37)</sup>. However due to the simplicity of the flow field and the accuracy of the CFD simulation, Fluent's NO<sub>x</sub> post processor was run and a 7 reactor CRN model was also generated. The NO<sub>x</sub> exit predictions from the CRN were within 5% of the NO<sub>x</sub> predictions from the Fluent NO<sub>x</sub> post processor.

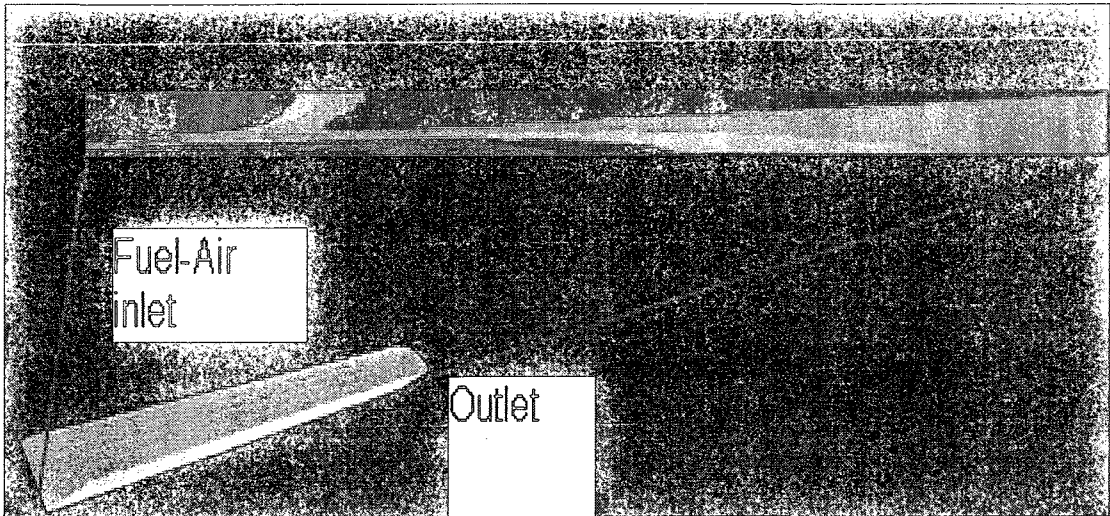


Figure 5-1: Lockwood CRN on Fluent

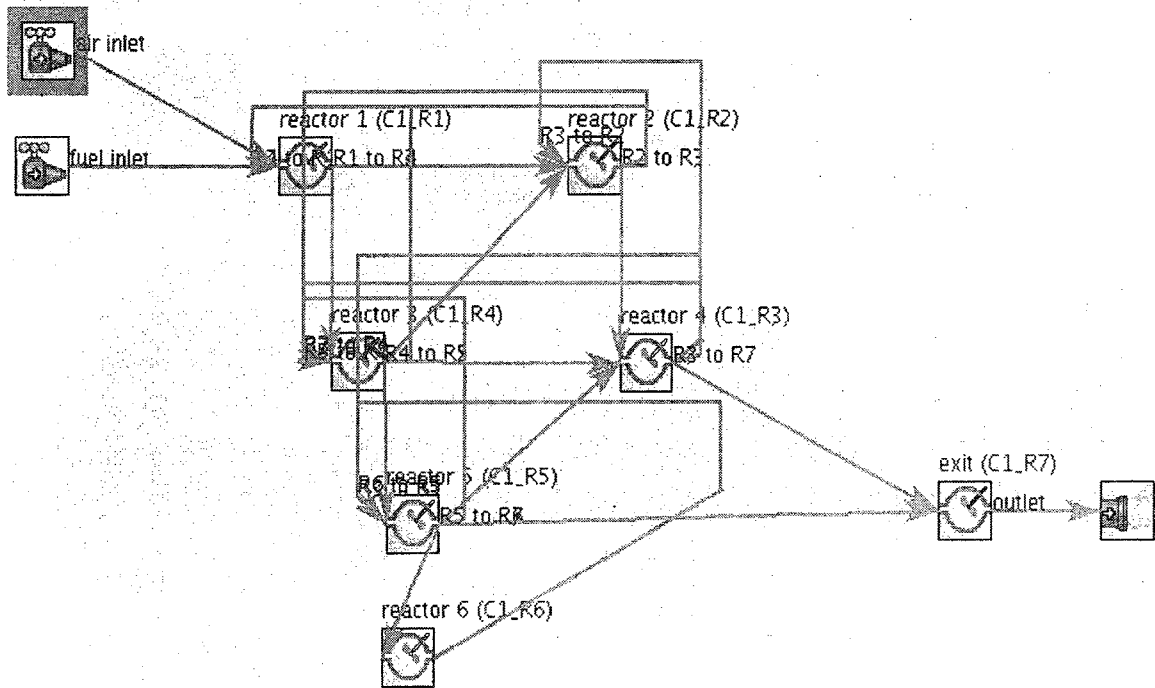


Figure 5-2: Lockwood CRN on Chemkin

The CRN above was the first attempt at creating a reactor network. Time constraint did not allow the author to extensively investigate and validate the method on Lockwood's geometry. Several other CRNs were generated during which a sensitivity analysis and debugging of the method was successfully done.

## **5.2 CRN Simulation of the RB211 Combustor's 45 Degree Slice**

The RB211 combustor's 45 degree slice of the primary zone was the first complex CFD model run and it was used as a benchmark to further develop and scrutinize the method used for CRN generation. Later a 45 degree slice of the entire RB211 combustor (with straightened discharge nozzle and most of the externals removed) was analyzed. The aim was to simplify the flow field and the number of cells for better analysis of the results. Soon new challenges regarding complex geometry analysis surfaced such as exclusion of the premixers and injectors from the bulk flow. The RB211 was at one point simulated with the premixer and the entire array of fuel injections. These created unnecessary volumes which would not be of interest to the author for CRN generation. Several attempts were made at simulating the entire 45 degree combustor with inlet profiles (velocity, temperature, mixture fraction etc...) read in directly from iso surfaces created on the 360 degree full combustor with the premixer attached. These inlet profiles would be read in only where the flow entered the bulk flow of the combustor. Fluent showed difficulties in obtaining convergence when a large number of inlet profiles were



interpolated. Therefore, an elaborate method of using ZoI, temperature and mixture fraction discretization was used to keep the premixer volumes out of the generated CRN.

Since there were no  $\text{NO}_x$  measurements available to us for the premixed case of RB211, the RB211's 45 degree slice was only used for debugging and development purposes.

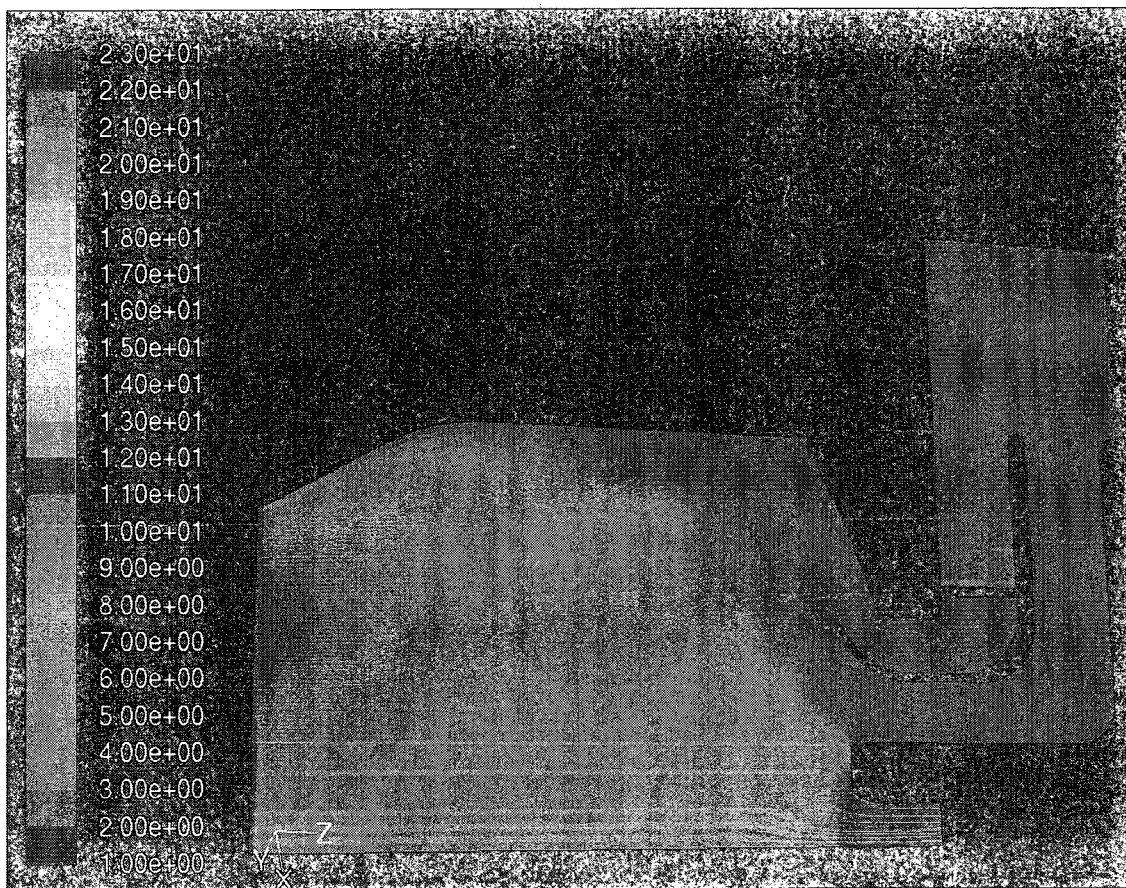
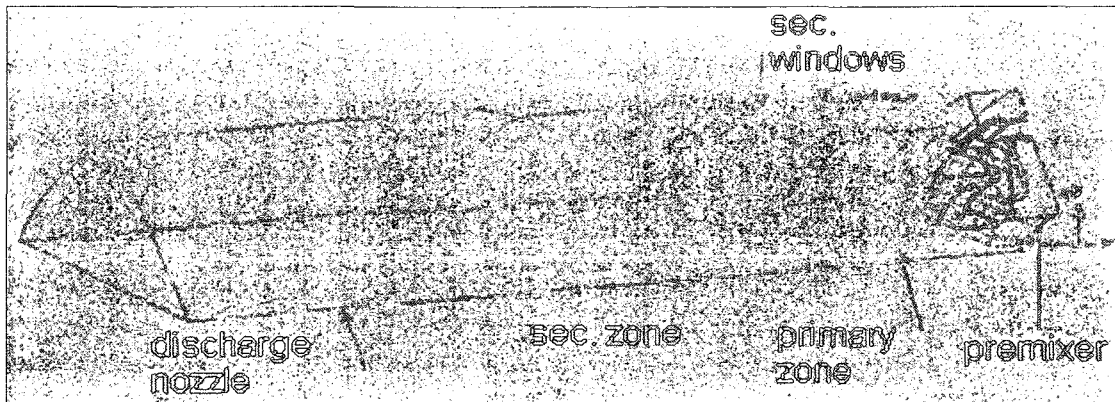


Figure 5-3: Sample RB211 Pie slice CRN



*Figure 5-4: Sample extended RB211 Pie slice with straightened discharge nozzle*

The O radicals were traced as they take part in the major NO<sub>x</sub> producing mechanisms as Guo et al<sup>(18)</sup> define it as the most important species to contribute to NO<sub>x</sub> production in LP combustion. The O radicals in each region of the RB211's 45 degree section of the primary zone and were compared with the PDF generated averaged O radical concentration. It was noticed that the general trends of O radical concentrations between the CFD and CRN simulation were in accordance in regions away from the walls. This may be explained by the CRN's inability to take wall effects into account. Fig 5-5 shows the O radical trend in an 8 reactor CRN which was generated during a trial run. The reactor number in the CRN is defined by the last digit in the reactor's name. For example C1\_R1 indicates reactor one which is portrayed in blue on Fluent's GUI contour.

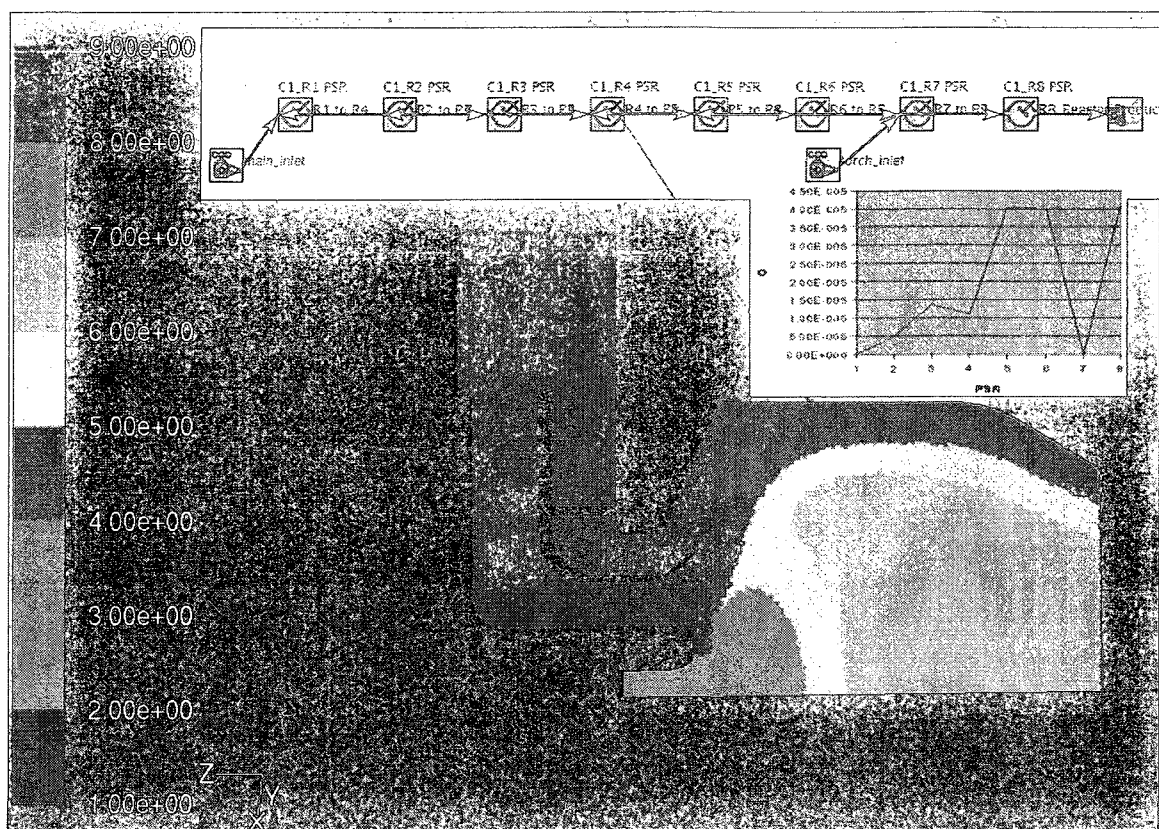


Figure 5-5: RB211 CRN-species concentration

The blue reactor simply represents one inlet and the orange reactor represents another inlet. Notice that the inlets and premixers are simulated via low temperature short residence time reactors since the assumption is that no reactions could occur in them. In Fig 5-5, the CFD analysis showed a considerable amount of cooling air entering the flame region however it seriously underestimated the amount of radicals entering the flame from the sides. The CRN simulation picked where the CFD was inadequate and calculated a higher concentration of the radicals entering the core of the flame from the sides. This could explain the complex stable nature of the combustion phenomenon in RB211 combustors. The flame seems to be slightly suppressed by the right amount of the

cooling air which also augments it by feeding it ready-to-react radicals. If accurate, the flame is being controlled by a push and pulls mechanism.

The major species are averaged for each reactor in CFD and compared with the CRN predictions. As mentioned before, for a well validated CFD solution, the PDF method is believed to predict the major species with reasonable accuracy. Therefore, the major species' concentrations obtained from the CFD are compared with the major species' concentrations obtained from the CRN. It is believed if the concentrations of the major species correspond between CFD and CRN, there will be confidence in the predictions of the CRN regarding the minor species.

Despite significant improvements in CRN generation obtained from the simple geometry simulations and increased understanding of the chemical reactions, these initial studies regarding the CFD CRN predictions of the major species were halted as instructed by the sponsoring organization.

### **5.3 CRN Simulation of the Full RB211 Combustor**

6 Fluent CFD files were received from Rolls Royce Canada to be examined against the experimental data. The 6 cases which generally vary in temperature field were singled out

from a series of experiments. Therefore the case numbers, which were previously labeled by their ID number, are kept as the original ones in all the tables which follow. The cases and their temperature field are presented in Table 1. For more information on the inlet boundary conditions and the flow field see Ref 28.

CASE 1	CASE 2	CASE 4	CASE 5	CASE 6	CASE 8
TPZ= $T_{ref}+50$ (K)  $T_{ex}=T_{ref}$ (K)	TPZ= $T_{ref}+50$ (K)  $T_{ex}=T_{ref}+125$ (K)	TPZ= $T_{ref}$ (K)  $T_{ex}=T_{ref}+125$ (K)	TPZ= $T_{ref}+50$ (K)  $T_{ex}=T_{ref}$ (K)	TPZ= $T_{ref}+50$ (K)  $T_{ex}=T_{ref}+125$ (K)	TPZ= $T_{ref}$ (K)  $T_{ex}=T_{ref}+125$ (K)
Natural Gas	Natural Gas	Natural Gas	Natural Gas + Ethane	Natural Gas +Ethane	Natural Gas + Ethane

*Table 1: A summary of the cases which were analyzed*

The 6 cases were chosen since they cover a range of flow fields with different thermal and composition properties. TPZ refers to the temperature in the primary zone and  $T_{ex}$  refers to the exit temperature of the combustor. The complex flow fields and the limitations of Chemkin posed a challenge in generating a reactor network which would closely represent the flow field while avoiding convergence issues. In order to have similar reactor networks for comparison, the reactor networks varied from 16-19 elements depending on the temperature range and gradients in each case. The size of the reactor network ensured consistency between each reactor network for further analysis while enhancing convergence in each case. The boundary conditions were taken accordingly from the CFD simulations.

Fig 5-6 is a representation of a 16 reactor CRN (15 PSRs + 1 PFR) generated on an averaged LES simulation. Reactors 1 and 2 are displayed with the red arrow. These volumes correspond to the regions which provide the secondary and primary zones with fuel and air. As Noticed the fuel and air enter one PSR reactor which indicates 100% prefect mixing. This is not exactly the case in real life. Novosselov <sup>(38)</sup> has proposed the use of several PSRs with a variation in composition to simulate a more realistic level of mixing.

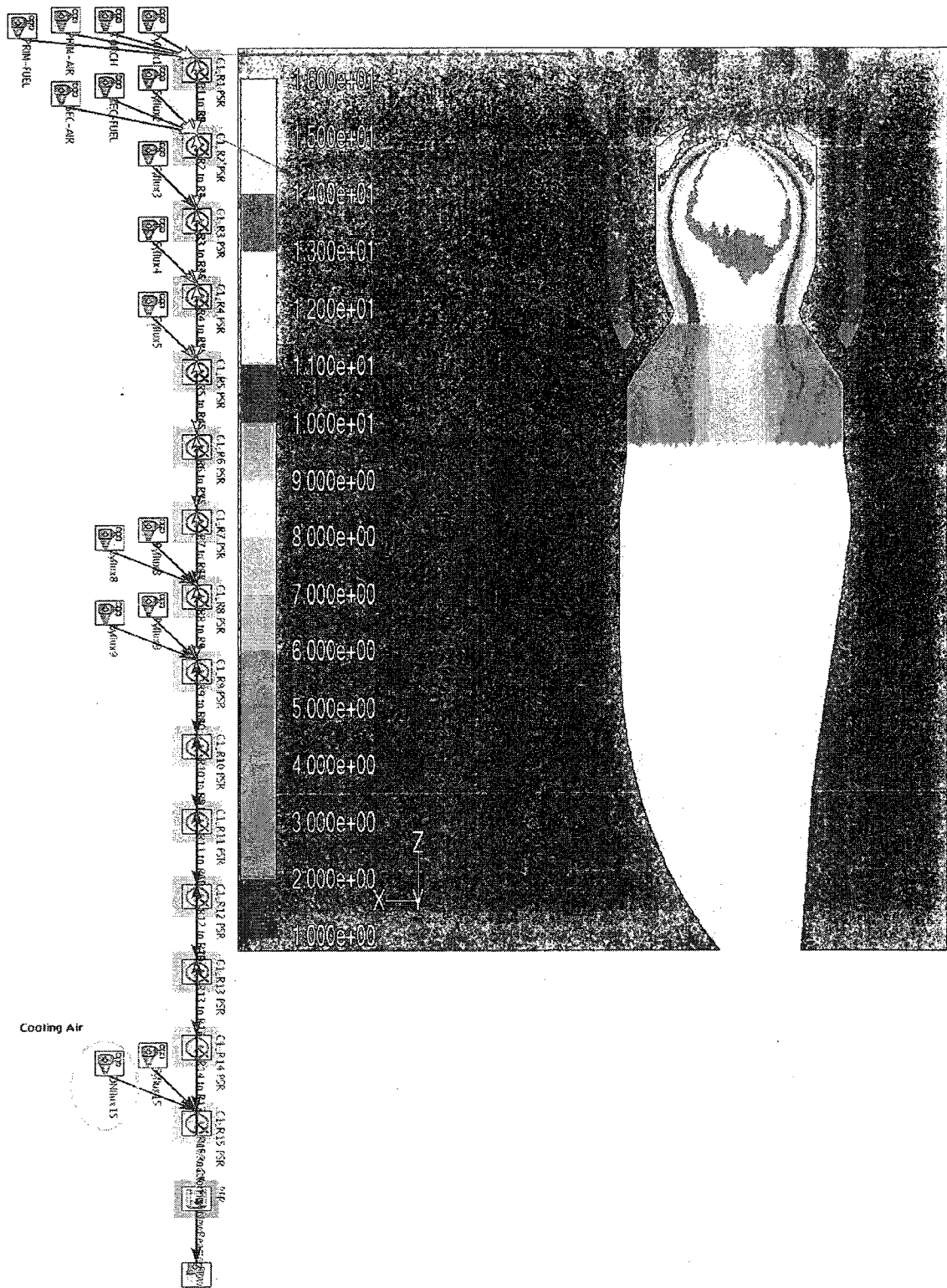
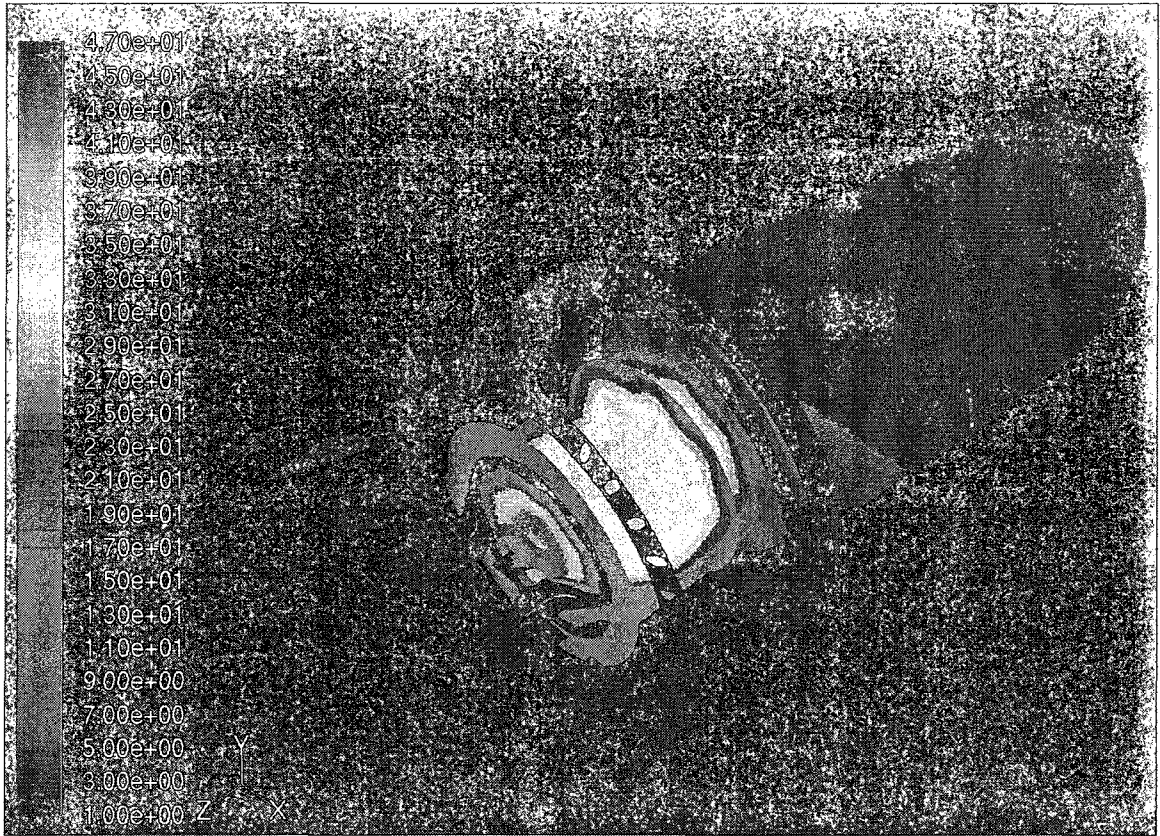


Figure 5-6: CRN on Fluent GUI and Chemkin



*Figure 5-7: Sample of 3D complex full RB211 combustor's CRN*

The image above is a comprehensive 3D representation of the reactors generated (and represented by distinct colors) in a full RB211 geometry. The regions in dark blue mainly comprise the non bulk flow regions which are not of interest and therefore have been dealt with accordingly.



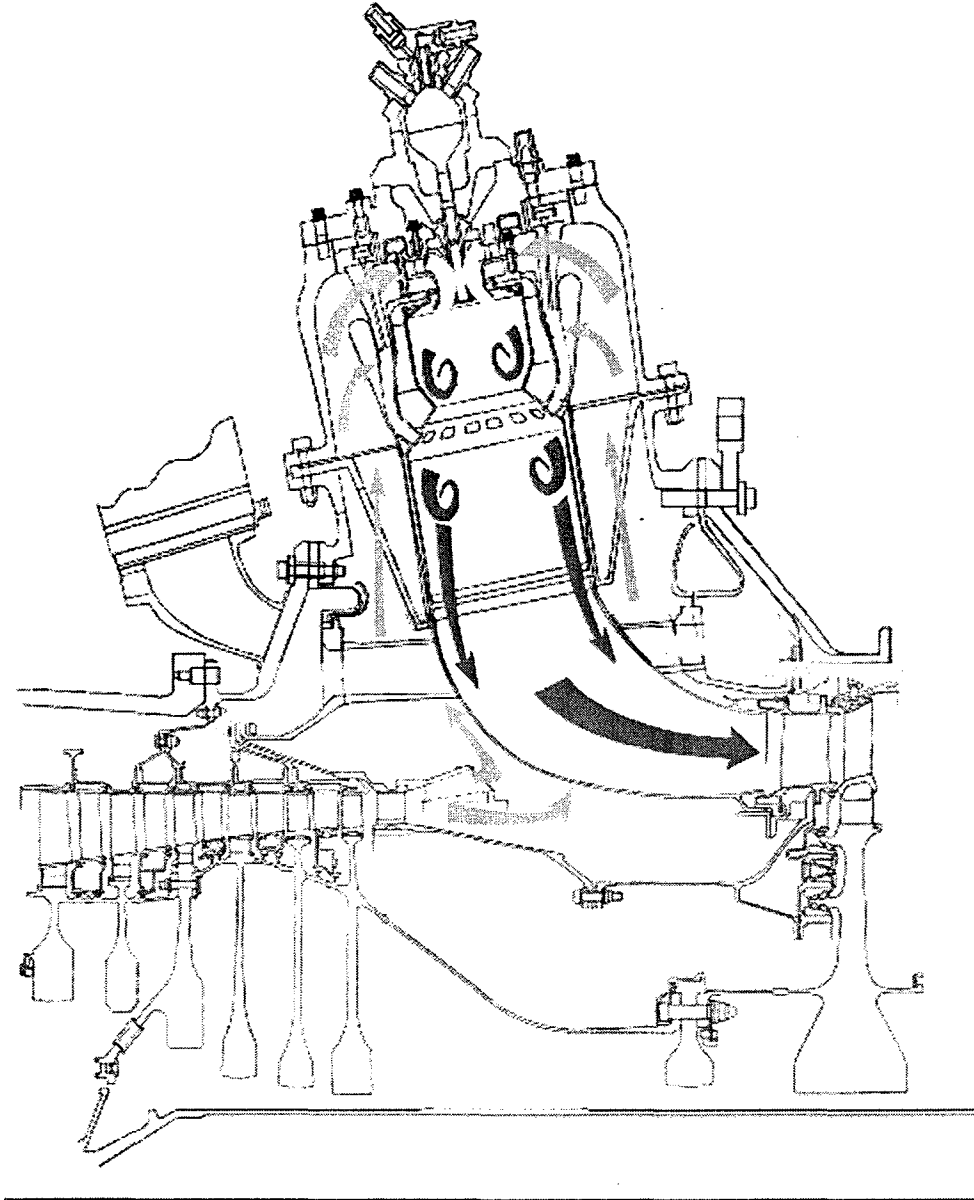


*Figure 5-8: RB211 Combustor schematic (Ref 39)*

The image above <sup>(39)</sup> is a general representation of an RB211 combustor which shows the main flow paths and the major vortices in the combustor in a schematic way.

## 5.4 **NO<sub>x</sub> Emission**

The NO<sub>x</sub> values were in general all roughly about one order of magnitude lower than the experimental values. The trend of the exit NO<sub>x</sub> emissions have been shown in Fig 5-9 against the experimental measurements. The CRN results do not show a trend similar to the experimental trend of the NO<sub>x</sub> values. The NO<sub>x</sub> results show little sensitivity to the variation of conditions in each case. However trials on the temperature field of the reactor network showed the NO<sub>x</sub> to be highly sensitive mainly to reactors at very high temperatures exceeding 1800 degrees Kelvin. This was observed as the temperature in the reactors around the flame was artificially increased in a sensitivity analysis. It is therefore necessary to generate a reactor network at higher resolutions especially around the flames to ensure accuracy in NO<sub>x</sub> results. It must be kept in mind that reactor network generation depends heavily on the resolution of the flame thickness. Typically, it is less than the filter width on the LES simulation. Moreover, the CRN network needs to agglomerate cells in order to avoid a large number of reactors which results in more artificial thickening. This corresponds to the trials made in a preliminary analysis. The flame can be represented with reactor networks of various sizes in order to understand the sensitivity of emissions to temperature gradients around the flame. The user can also manually adjust the temperatures in each reactor and note down the response of the reactor network to any change in temperature and residence time. Previous preliminary examination of the reactor networks showed that the network only responded to temperature variations which were about 1800 degrees Kelvin and higher. However, a thorough study of the flame and emission dependence on temperature is required before

any conclusion could be drawn.

The way forward then, would be to refine the reactors at the flame-front. In order to avoid the flame-front thickness produced in CFD, the reactor filters can be refined in order to create reactors that are biased towards a thinner flame-front – perhaps by homogenizing the surrounding temperature zones in the neighboring reactors and iterating against experimental data until a match is obtained. It is believed that a large number of reactors need to be concentrated around the hot zones to ensure reliable predictions of  $\text{NO}_x$ . A thorough sensitivity analysis regarding the concentration of reactors required to capture  $\text{NO}_x$  and to track the species in each reactor is the subject of future research.

CASE	RATIO	$\text{NO}_x$ (ppmv)
1	CASE1/CASE1=1	--Proprietary Info--
2	CASE2/CASE1=1.38	--Proprietary Info--
4	CASE4/CASE1=1.035	--Proprietary Info--
5	CASE5/CASE1=0.82	--Proprietary Info--
6	CASE6/CASE1=1.02	--Proprietary Info--
8	CASE8/CASE1=0.54	--Proprietary Info--

*Table 2: It represents the  $\text{NO}_x$  values and the normalization of  $\text{NO}_x$  values based on Case1*

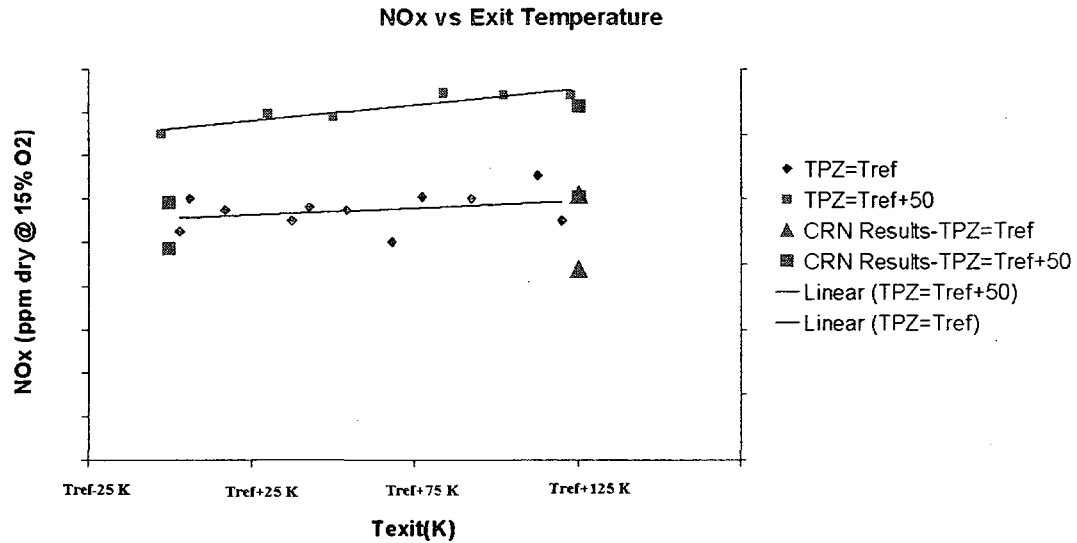


Figure 5-9: CRN and experimental  $NO_x$  values

In Fig 5-9 TPZ refers to the temperature in the primary zone of the combustor. The y axis on the right corresponds to the CRN results and the y axis on the left corresponds to the rig data. (Values are removed due to Copy Right compliance).

Fig 5-9 is a representation of the CRN generated  $NO_x$  predictions against the experimental values for the 6 cases described in Table 1. Case 2, Case 4 and Case 6 which have higher exit temperatures compared with Case 1 and Case 5 show consistently higher values of  $NO_x$  as expected. However Case 8's exit  $NO_x$  is estimated to be lower than Case 1 and Case 5 even with a higher exit temperature. It is believed that such inconsistencies (as in Case 8) would be eliminated with more complex reactor networks which would be more representative of the combustion flow field. It is vital to capture much smaller temperature gradients to see noticeable response from  $NO_x$  production

source terms. The addition of ethane ---Proprietary Info--- to show a noticeable change in the NO<sub>x</sub> results as ---Proprietary Info--- by the rig data.

NO<sub>x</sub> formation highly depends on temperature and residence time. Its formation rate at high temperatures increases exponentially therefore necessitating temperature regulation to manage the emissions. It is always a challenge to strike a balance between CO and NO<sub>x</sub> formation since they generate rapidly under opposite conditions.

## **5.5 CO Emission**

The CRN results for CO showed large variations as seen in Table 3. However, Case 2, Case 4, Case 6 and Case 8 have CO values under 100 ppmv which are considerably lower than the CO obtained from Case 1 and Case 5. Case 2, Case 4, Case 6 and Case 8 all share a hotter discharge nozzle which seems to reduce the CO levels considerably. The slight jump in the CO level in case 8 could be simply attributed to the reactor arrangement and inadequate capturing of hot temperature zones. Table 3 indicates that CO is highly sensitive to any changes in temperature at the discharge nozzle since the cases with higher exit temperature have significantly lower CO compared with the cases with lower exit temperature. Therefore CO shows a higher sensitivity to exit temperature than NO<sub>x</sub> as shown in the previous section. A higher concentration of reactors is expected to eliminate the discrepancies and generate more accurate results. In case of wall quenching,

a higher resolution of reactor would be required at the walls for CO calculations. However, this is subject to future studies since ideal reactors can not take boundary layers (wall effects) in to account due to their mathematical nature and a more developed algorithm is required for very large reactor networks.

CASE	RATIO	CO (ppmv)
1	CASE1/CASE1=1	--Proprietary Info--
2	CASE2/CASE1=0.0031	--Proprietary Info--
4	CASE4/CASE1=0.00728	--Proprietary Info--
5	CASE5/CASE1=1.405	--Proprietary Info--
6	CASE6/CASE1=0.0164	--Proprietary Info--
8	CASE8/CASE1=0.0794	--Proprietary Info--

Table 3 represents the CO values and the normalization of CO values based on Case1

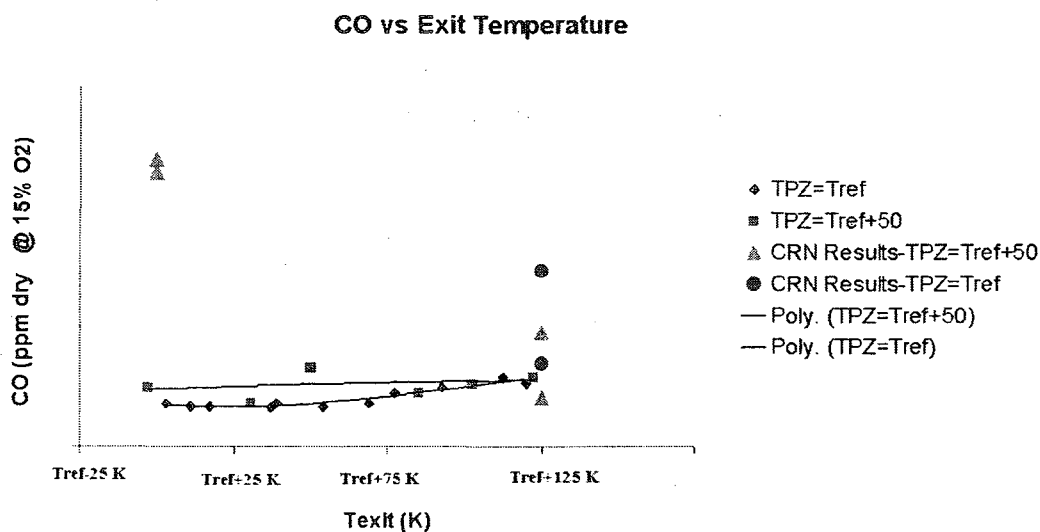


Figure 5-10: CRN and experimental CO values

In Fig 5-10, the green triangles and the red circles represent the CO values obtained from the corresponding CRNs. A Log scale was used since Case 1 and Case 5 generate unreasonably high CO.

## **5.6 Summary**

The first CRN, comprising of 7 reactors, was created on a simple combustor and  $\text{NO}_x$  value obtained from the CRN simulation at the exit of the combustor was within 5% of the CFD predicted  $\text{NO}_x$ . Later a 45 degree slice of the RB211 primary zone was discretized into a CRN and the  $\text{NO}_x$  values predicted by the CRN were within 10% of the experimental measurements.

Finally, 6 LES simulations of the full RB211 combustor with various boundary conditions were analyzed via 6 different CRNs ranging from 16-19 reactors depending on the CFD temperature ranges. Consistent under prediction of  $\text{NO}_x$  and some over prediction of CO at the exit of the combustor are mainly attributed to the use of small CRNs and neglecting of temperature fluctuations. Larger CRNs could not be used due to Chemkin's limitations, however the 6 cases were run in accordance with the agreement with Rolls Royce Canada.

## 6 CONCLUSION

A method of producing chemical reactor networks has been devised based on the CFD results obtained from Fluent. Initial obstacles were faced with regards to the computation time required for generating CRNs. Several improvements were made to enhance the processing time of the UDF from days to minutes. The current project has been able to introduce an optimized methodology for reactor network generation based on previous research publications. A semi automatic algorithm has been developed for direct extraction of CRNs from CFD flow fields. The optimized CRN approach and the robust algorithm would allow highly accurate CFD based CRNs to be generated within minutes. As CRNs are robust and capable of predicting species' concentrations, emissions predictions could be implemented via a personal computer within minutes; a task which would have taken months if not years via conventional CFD methods.

Further studies are advised starting from simple premixed geometries. The most challenging part of generating CRNs is on non premixed flames where high temperature and composition gradients require high reactor density. On the other hand, premixed flames provide smooth variation in temperature and composition therefore easing the task of CRN generation. Considering that the simulation of premixed flames has also proven to be more challenging compared with diffusion flames, the relative ease of CRN



generation on premixed combustion would be most valuable to the industry and to the academic society.

During the course of this investigation several other aspects of CRN generation for future enhancement of the current algorithm have been researched. Discretization of the flow field based on turbulent kinetic energy and eddy turnover time was partially studied. The study was mainly with regards to diffusion flames where mixing and its relation to reactor type become of great importance. Unmixedness indices, temporal and spatial standard deviations of mixture fraction and temperature were studied to investigate any possibility of defining the reactor type in non premixed combustors where mixing is of great significance. Almost in all cases some level of correlation was discovered, however further studies on well validated geometries will be implemented in order to validate any findings. There is currently no guaranteed way of defining the reactor types in certain non premixed combustors. Engineering judgment or the direction of the velocity field has traditionally been used to determine the suitable reactor type for a specific flow region. Where velocity angle gradients were high, engineers would automatically assume high levels of turbulence and therefore PSR behavior. Complex industrial combustors with non linear geometries and flame controlling recirculation zones, where thermal and composition gradients vary significantly across recirculation zones, render the traditional approaches for defining the reactor types impractical. For example, a large velocity gradient could simply indicate geometric non linearity in a modern combustor geometry and may not indicate PSR behavior in that specific region. Definition of reactor type based on velocity angle gradients is inaccurate and impractical. Further studies are required to devise a reliable method of defining the reactor types via new methods such

as the second temporal and spatial variances of mixture fraction and temperature. These studies were not completed as the current thesis is focused on the RB211 partially premixed combustor and well mixed flow fields are generally represented with PSRs.

Some of the past difficulties such as conservation of mass flow in each reactor, geographical discretization and calculation of residence times were tackled and an automatic method of generating input files to Chemkin was incorporated. Although the developed UDF is for use on Fluent and requires further work, the underlying programming techniques and engineering methods can be applied to any other in-house or commercial CFD soft wares. The current methods and achievements can be generally summarized as follows;

- Discretization of flow field based on their geographical location, mixture fraction and temperature (other parameters could easily be incorporated as well)
- Rapid generation of reactor networks (within minutes) extracted from CFD flow field
- Obtaining conserved mass flow within each reactor – no need to ‘guesstimate’ it.
- Automatic averaging of temperature and composition in each reactor
- Automatic simplification of flow field reactor network based on the user’s input
- Automatic generation of the reactor data into a Chemkin format
- Accounting for cooling air influence

- Graphical representation of the reactors on the CFD

6 chemical reactor networks were generated (from Fluent CFD case files) to represent the RB211 combustor with different temperature and flow fields (see section 5.3). Although the  $\text{NO}_x$  was under predicted consistently, CO predictions showed results which varied considerably according to the temperature field and the flow fields. There was some agreement between the CRN and experimental values on CO for certain cases. The hotter temperature fields seemed to predict results which were within the reasonable range, while the colder temperature field over predicted the CO production.

It is believed that the accuracy of the results could be improved in three principal ways;

- Refinement of reactor resolution (increase of reactor numbers) within the combustor especially around the flame and a more extensive use of non PSR reactors (such as PFR, PaSR, MIXERs etc...) via more robust soft wares.
- Incorporation of temperature correction factors due to the steady state assumption on the temperature field.
- Tracking of influential species such as O and OH in each reactor and validation against experimental data in order to find any sources of inaccuracies.

## 6.1 Future Work

An important and challenging task ahead is to use an alternative soft ware (except for the current version of Chemkin 4.1) that *allows* the user to integrate various types of reactors (using an input file) and connections (such as PSR, PFR, MIXERs etc...) to obtain an accurate representation of the flow field. At first, a large reactor network needs to be generated with a large number of PSRs in order to guarantee homogeneity in each PSR. Then every few PSRs could be replaced by the corresponding alternative reactor (such as PFR, PaSR etc...) where the flow properties allow.

It is of great significance to conduct the analysis of temperature fluctuations on  $\text{NO}_x$  and CO. It is believed that the steady state assumption of temperature could result in considerable under prediction of  $\text{NO}_x$  and inaccuracies in CO calculations<sup>(32, 40)</sup>. This is consistent with the under predicted  $\text{NO}_x$  values obtained before. An analysis for the correction of temperature in the reactor network is recommended in order to incorporate the effect of temperature fluctuations on the emissions. The temperature fluctuations and consequently the residence time fluctuations can be taken into account via a temperature correction factor. The temperature variance in each cell could be found based on its mixture fraction via the PDF table. It has been noted that for example as a general rule of thumb, on the RB211 Pie slice, that the addition of 75% of the variance of temperature to the averaged temperature results in reasonable prediction of  $\text{NO}_x$  and CO emissions.

Another task ahead is to continue studying the main species' trends (such as OH and O, CO, NO etc...) in each reactor and to compare them with the results obtained from CFD or preferably from the experiments. The comparison would be highly beneficial in determining the reasons for the deviation of the numerical results from those of the experiment. The species' mole fractions averaged for every reactor can be plotted and compared against Chemkin's calculated species' mole fractions. This approach has been examined on a preliminary basis where a 45 degree of the RB211 was used for the generation of a chemical reactor network. The general trends of the O and OH radicals obtained corresponded qualitatively around the flame between the CFD and the CRN, although they slightly differed in their quantities. It is believed a more thorough analysis and tracking of species is required in order to tackle the source of inaccuracies in chemical reactor networks

The effect of non homogeneity (circumferentially and radially) of fuel air mixture at the inlet could also be simulated by representing the inlet with more than one PSR. The series of PSRs could have slight variation in mass flow rate, temperature and mixture fraction.

Following the end of the current project, Reaction Design has introduced its new version of Chemkin called Chemkin Pro. This software claims to have removed a few limitations such as the number of PSR-PSR connections. They also claim to have a significantly more robust solver with much better convergence capabilities. It is highly recommended to examine this software in the future.

## 6.2 Contribution to Knowledge

A practical methodology based on previous literature and the available tools and softwares has been presented for the coupling of CFD-CRN for cost effective prediction of polluting emissions. The methodology which is partially based on CFD results has been implemented on a complex industrial combustor in order to discuss the strengths and the limitations of CRNs and their range of applicability. It has been shown that efficient generation of CRNs for further research could be done with some programming in the form of a UDF coupled with mainstream commercial CFD and chemical kinetics softwares or any in house code.

Emissions prediction and sensitivity analysis could be potentially implemented on personal computers in a matter of minutes and hours instead of weeks and months. Although this thesis is not concerned about the CFD aspect of the work, some CFD tips and techniques have been discussed to facilitate numerical convergence and CRN development even on complex geometries.

Future steps for the completion of this work have been discussed (see Section 6.1). The need for higher resolution of the reactor networks and the necessity for more elaborate solvers have been articulated. The author strongly believes that with further research on the current advancements, most combustion phenomena and even other types of reactions can be analyzed in detail via the presented methodology.

## REFERENCE

1. Health Effects of Air Pollution. [http://www.hc-sc.gc.ca/ewh-semt/air/out-ext/effe/health\\_effects-effets\\_sante\\_eng.html](http://www.hc-sc.gc.ca/ewh-semt/air/out-ext/effe/health_effects-effets_sante_eng.html). (2008).
2. Ozone Transport Commission (OTC) NO<sub>x</sub> Budget Program. <http://www.epa.gov/airmarkt/progsregs/nox/otc.html>. (2008).
3. Kyoto Protocol. [http://unfccc.int/kyoto\\_protocol/items/2830.php](http://unfccc.int/kyoto_protocol/items/2830.php). (2008).
4. "Air Pollution". [http://www.who.int/topics/air\\_pollution/en/](http://www.who.int/topics/air_pollution/en/). (2008).
5. Falcitelli, M. Pasini, S. Tognotti, L., Modeling Practical Combustion Systems and Predicting NO<sub>x</sub> Emissions with an Integrated CFD Based Approach. *Computers and Chemical Engineering*. **26**, 1171-83. (2002).
6. Novosselov, I.V., Eight Step Global Kinetic Mechanism on Methane Oxidation with Nitric Oxide Formation for Lean Premixed Combustion Turbines. *ASME Turbo Expo*. **2**; 769-779. (2007).
7. Novosselov, I.V., Malte, P.C., Development and Application of an Eight Step Global Mechanism for CFD and CRN Simulations of Lean Premixed Combustors. *ASME*. (2008).

8. Falcitelli, M. Tognotti, L. Pasini, S., An Algorithm for Extracting Chemical Reactor Network Models from CFD Simulation of Industrial Combustion Systems Combustion Science and Technology. 27-42. (2002).
9. Kee,R.J., Coltrin,M.E., Glarorg, P., Chemically Reacting Flow : Theory and Practice. John Wiley and Sons, Canada. (2003).
10. Annamalai,K., Puri, I.K., Combustion Science and Engineering, Taylor and Francis.U.S.A.(2007).
11. Biagioli,F.,Guthe,F., Effect of Pressure and Fuel–Air Unmixedness on NO<sub>x</sub> Emissions from Industrial Gas Turbine Burners. Combustion and Flame, **151**, 274-288. (2007).
12. Chemkin User Guide. Reaction Design, USA. (2007).
13. Rutar, T., Horning, D.C., Lee, J.C.Y., Malte, P.C., NO<sub>x</sub> Dependency on Residence Time and Inlet Temperature for LP Combustion in JSRs. ASME.9p GT. (1998).
14. Rutar,T., Malte, P.C., NO<sub>x</sub> Formation in High Pressure Jet Stirred Reactors with Significance to Lean Premixed Combustion Turbines. AMSE Transactions. **124**. (2002).



15. J. O. Keller, T. T. Bramlette, P. K. Barr, and J. Alvarez., NO<sub>x</sub> and CO Emissions from a Pulse Combustor Operating in a Lean Premixed Mode. Sandia National Laboratory. Presented at the Western States Section. Combustion Institute Spring Meeting, University of Utah, Salt Lake City, Utah. (1993).
16. Baukal, C.E., The John Zink Combustion Handbook (Industrial Combustion Science). John Zink Co., USA. (2000).
17. University of California at Berkeley. <http://www.me.berkeley.edu/gri-mech/releases.html>. (2007-2008).
18. Guo, Honsheng., A Numerical Study on NO<sub>x</sub> Formation in Laminar Counterflow CH<sub>4</sub>/air Triple Flames. *Combustion Modeling and Theory*.**11**. 741-53.(2007).
19. Steele,R.C., Malte,P.C.,Nicole,D.G., Kramlich, J.C., NO and N<sub>2</sub>O in Lean-Premixed Jet-Stirred Flames. 24<sup>th</sup> Symposium on Combustion, **100**;3,440-449,California. (1995).
20. Bragg, S.L.,Application of Reaction Rate Theory to Combustion Chamber Analysis. Aeronautical Research Council Pub. ARC 16170, Ministry of Defense, London, U.K, 1629-1633. (1953).
21. Swithenbank, J., Combustion Fundamentals. *AFOSR 70-2110 TR*, (1970).

22. Schlegel, A., Benz,P., Griffin, T., Weisenstein, W., Bockhorn, H. Catalytic Stabilization of Lean Premixed Combustion : Method for Improving NO<sub>x</sub> emissions. Combustion and Flame. **105-3**, 332-240. (1996).
23. Ehrhardt,K., Toqan,P., Jansohn.p., Teare,J.D., Beer. J.M.,Sybon, G., Leuckel. W., Modeling of NO<sub>x</sub> Reburning in a Pilot Scale Furnace Using Detailed Reaction Kinetics. Combustion Science and Technology,**131**, 131-146. (1998).
24. Levenspiel,O., Chemical Reaction Engineering.Wiley and Sons.(1998).
25. Andreini, A., Facchini,B., Gas Turbine Design and Off-Design Performance Analysis with Emissions Evaluation. ASME. 83-91. (2004).
26. Bitondo, D. Rolls-Royce internal report. (2007).
27. Kuo, K.K., Principals of Combustion. 2<sup>nd</sup> Ed. John Wiley and Sons, Canada. (2005).
28. Jella, S.E., “Emissions Predictions in Turbulent Reacting Industrial Gas Turbine Combustor Flows using RANS and LES methods”. Concordia University. (2008).
29. Rubins,P.M., Pratt,D.T., Zone Combustion Model Development and Use:

- Application to Emissions Control. ASME. 1-8. (1991).
30. Pedersen,L.S, Breithaupt,P., Dam-Johansen, K., Weberb R., Residence Time Distributions in Confined Swirling Flames. Combustion Science and Technology.127:1, 251-273. (1997).
31. Mohamed. H.,Ticha,B.H., Sassi,M., Simulation of Pollutant Emissions from a Gas Turbine Combustor. Combustion Science and Technology. 176-5, 819-834. (2004).
32. Novosselov,I.V., Chemical Reactor Networks for Combustion Systems Modeling, University of Washington, USA. (2006).
33. Rolls Royce Internal Report. G.Hesami, Sam. (Aug 2007).
34. Fluent User Defined Function manual. Fluent Inc, USA. (2006).
35. Rolls Royce Internal Report. G.Hesami, Sam. (May 2008).
36. Mr K Brundish, K.,Miller, M., RB211 DLE Combustor Internal Traversing. Qinetiq, U.K.,. (2001).
37. Lockwood, F.C.,El-Mahallawy, F.M., Spalding, D.B., An Experimental and

Theoretical Investigation of Turbulent Mixing in a Cylindrical Furnace. Combustion and Flame .23-3, 283-293. (1974).

38. Novosselov, I.V. Malte, P.C.; Yuan, S.; Srinivasan, R.; Lee, J.C.Y., Chemical Reactor Network Application to Emissions Prediction for Industrial DLE Gas Turbines. Proceedings of the ASME Turbo Expo, v 1, Proceedings of the ASME Turbo Expo - Power for Land, Sea, and Air. 221-235. (2006).
39. Eggels. R.L.G.M., Modelling of NO<sub>x</sub> Formation of a Premixed DLE Gas Turbine. Proceeding of Turbo Expo, 46<sup>th</sup> ASME International Gas Turbine and Aeroengine Technical Congress. New Orleans, Louisiana, USA. (2001).
40. Habib,M.A., Elshafaei,M. Computer Simulation of NO<sub>x</sub> Forming in Boilers. King Fahd University of Petroleum and Minerals. Saudi Arabia.

## APPENDIX A-FLUX CALCULATIONS

The fluxes are extracted directly from the CFD field via the macro F\_FLUX. The validity of this macro was examined after correspondence with Fluent USA. A separate UDF was written to compare the F\_FLUX performance at the boundaries with the direct calculation of the flux terms at the boundaries where the exact flux is known. The dot product of velocity vectors and face normal vector at the boundary faces were obtained and compared with the F\_FLUX values and they corresponded exactly therefore ensuring the validity of using this macro.

The case was also tried on the Lockwood<sup>(37)</sup> combustor by dividing the geometry into two zones right after the corner recirculation zone to avoid the effect of reverse flow as much as possible. The Lockwood combustor was selected due to its simplicity compared with the RB211. The Lockwood combustor acts similar to a plug flow reactor at a distance from the inlets. Therefore the total mass flow rate at the inlet is expected to be equal to the mass flow rate at a cross section further downstream. The difference between the net mass flux across the cross section calculated by the *CRN Generator* and the total mass flow inlet was 0.003% which shows great correspondence and validity of the flux calculation method. The volumes of all reactors were also added (for Lockwood and RB211) and compared with Fluent's volume integral option for the entire geometry and they corresponded accurately.

## APPENDIX B-TRIMMING OF REACTORS

Due to the discretization parameters defined by the user, small reactors may form which may further complicate the CRN and pose numerical difficulties in obtaining convergence. Falcitelli et al <sup>(8)</sup> tackle this problem by regrouping the smaller reactors into larger reactors based on their level of unmixedness.

They define an unmixedness index for each reactor as follows;

$$Z_{TOTAL} = \frac{1}{N} \sum_{i=1}^N Z_i \quad \text{Equation B.1}$$

Where;

$$Z_i = \frac{\bar{Y}_i^2 - \overline{Y_i^2}}{\bar{Y}_i(1 - \bar{Y}_i)} \quad \text{Equation B.2}$$

$$\bar{Y}_i = \frac{\sum_j Y_{ij} \rho_j V_j}{\sum_j \rho_j V_j} \quad \text{Equation B.3}$$

$$\overline{Y_i^2} = \frac{\sum_j Y_{ij}^2 \rho_j V_j}{\sum_j \rho_j V_j} \quad \text{Equation B.4}$$

Each cell which is supposed to be regrouped into a new reactor is then arbitrarily reassigned into a neighbouring reactor and the increment is calculated via Equation 9.5.

$$(n + 1)Z_{TOT}^* - nZ_{TOT} = \text{increment} \quad \text{Equation B.5}$$

The reassignment which corresponds to the minimum value of the increment is permanently kept.

This method was shortly used in generating of a CRN via the mixture fraction as described below;

$$\tilde{f}''^2 / \tilde{f} / (1 - \tilde{f}) \quad \text{Equation B.6}$$

It must be noticed that as  $\tilde{f}$  tends to 1, the Equation 9.6 tends to infinity.

The regrouping approach was complicated and seemed to add little value to the CRN on a preliminary basis. The new regrouped cells would further extend the range of the temperature and composition over which the reactor properties were being averaged. This introduced further inaccuracies in the model. Since the number of unassigned cells was generally small it was decided to remove them for the initial studies as their very short residence times would barely have any effect on the kinetics calculations.

## APPENDIX C-CRN SIMPLIFIED

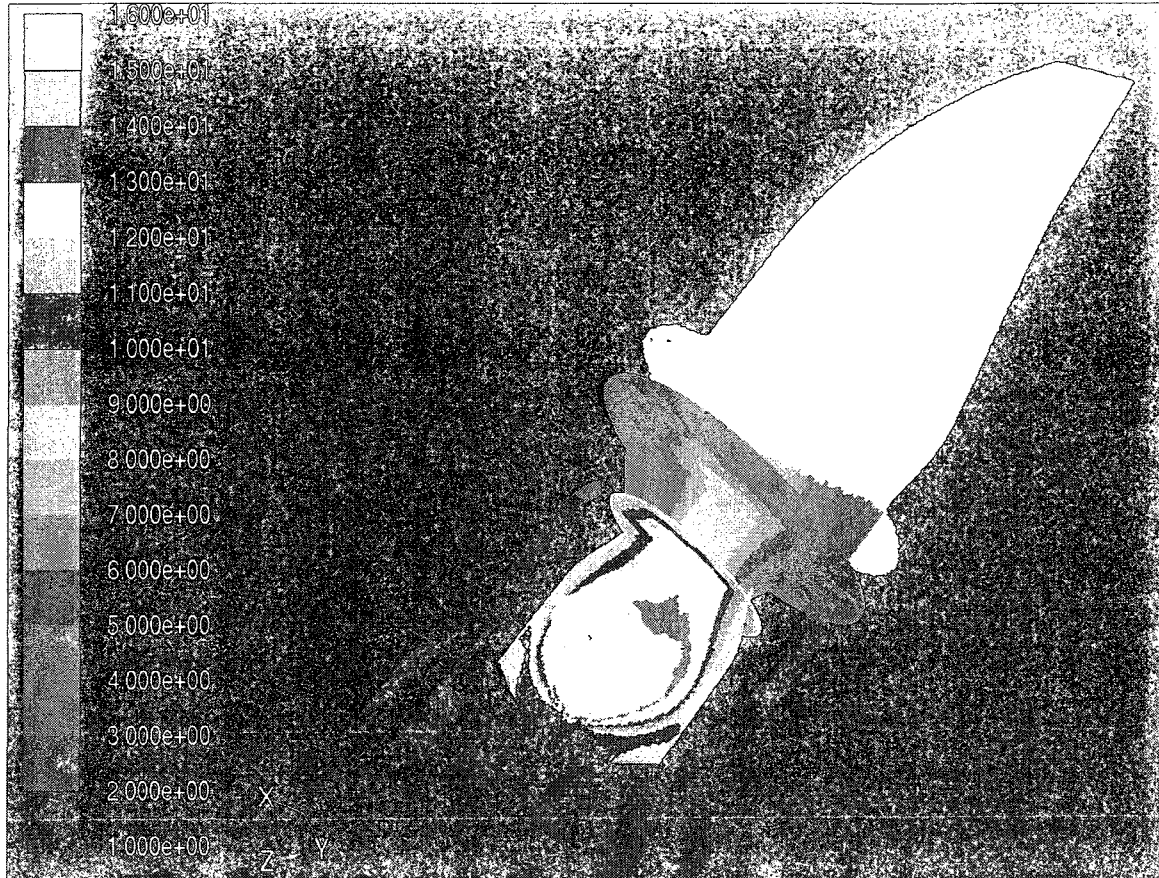


*Figure C-1: Depiction of reactors extracted from the CFD field*

A typical CRN with 15 reactors is displayed in Fig 9-1. The sum of each reactor's exit mass flow recycling fractions sums to 1 (except for the discharge nozzle reactor which mainly directs the flow into the exit). The first column indicates the donor reactor and the following rows indicate the receiver reactors and what percents of recycling mass flow they receive.



- Reactors 8,9,10,11,12,13 and 14 are in the primary zone
- Reactors 3,4,5,6 and 7 are in the secondary zone.
- Reactor 15 directs the flow to the exit and is the reactor representing the discharge nozzle
- Reactors 1 and 2 refer to the premixer